

**PROVENANCE STUDIES ON LIMESTONE ARCHAEOLOGICAL
ARTIFACTS USING TRACE ELEMENT ANALYSIS**

**A THESIS SUBMITTED TO
THE GRADUATE SCHOOL OF NATUREL AND APPLIED SCIENCES
OF
THE MIDDLE EAST TECHNICAL UNIVERSITY**

BY

ÜFCADE MUŞKARA

**IN PARTIAL FULFILLMENT OF THE REQUIREMENTS FOR THE
DEGREE OF
MASTER OF SCIENCE
IN
ARCHAEOMETRY**

MAY 2007

Approval of the Graduate School of Natural and Applied Sciences.

Prof. Dr. Canan ÖZGEN

Director

I certify that this thesis satisfies all the requirements as a thesis for the degree of Master of Science.

Prof. Dr. Asuman G. TÜRKMENOĞLU

Head of Department

This is to certify that we have read this thesis and that in our opinion it is fully adequate, in scope and quality, as a thesis for the degree of Master of Science.

Prof.Dr. Şahinde DEMİRCİ

Co-Supervisor

Prof. Dr. O. Yavuz ATAMAN

Supervisor

Examining Committee Members

Prof. Dr. Asuman G. TÜRKMENOĞLU (METU, GEOE) _____

Prof. Dr. O. Yavuz ATAMAN (METU, CHEM) _____

Prof. Dr. Şahinde DEMİRCİ (METU, CHEM) _____

Prof. Dr. Numan TUNA (METU, City Planning) _____

Prof. Dr. Mürvet VOLKAN (METU, CHEM) _____

I hereby declare that all information in this document has been obtained and presented in accordance with academic rules and ethical conduct. I also declare that, as required by these rules and conduct, I have fully cited and referenced all material and results that are not original to this work.

Name, Last name :

Signature :

ABSTRACT

PROVENANCE STUDIES ON LIMESTONE ARCHAEOLOGICAL ARTIFACTS USING TRACE ELEMENT ANALYSIS

Muşkara, Üftade

M.S., Department of Archaeometry

Supervisor : Prof. Dr. O. Yavuz Ataman

Co-Supervisor : Prof.Dr. Şahinde Demirci

May 2007, 61 pages

Trace element composition of archaeological artifacts is commonly used for provenance studies. Limestone has generally studied by geologists and there are a few researches done by various archaeological sciences. Although it is a common material for buildings and sculpture it is been thought that limestone used had not imported like marbles.

Limestone figurines from Datça/Emecik excavations are classified as Cypriote type, which was very popular through 6th century B.C. in the Mediterranean region. Since this type of figurines was found at Emecik numerously to determine its provenance was an important problem.

Emecik figurines were examined for their some major, trace elements and REE compositions and results were compared with geological samples which were

taken from a near by quarry. Inductively Coupled Plasma-Optical Emission Spectrometry (ICP-OES), Inductively Coupled Plasma-Mass Spectrometry (ICP-MS) have been used for analysis. The methods have been optimized by using standard reference material NIST 1d, NCS DC 73306, and IGS40.

Keywords: inductively coupled plasma – mass spectrometry, limestone, provenance, Cypriot figurines, REE.

ÖZ

ESER ELEMENT ANALİZİ İLE ARKEOLOJİK KİREÇTAŞI BULUNTULARIN HAMMADDE KAYNAĞININ SAPTANMASI ÇALIŞMALARI

Muşkara, Üftade

Yüksek Lisans, Arkeometri ABD

Tez Yöneticisi : Prof. Dr. O. Yavuz Ataman

Ortak Tez Yöneticisi : Prof.Dr. Şahinde Demirci

Mayıs 2007, 61 sayfa

Arkeolojik buluntuların eser element bileşimi, hammadde kaynağının belirlenmesine yönelik araştırmalarda sıklıkla kullanılmaktadır. Kireçtaşı genel olarak jeologlarca çalışılmış, ancak arkeolojik bilimlerin konusunu oluşturan sayılı inceleme bulunmaktadır. Yapı ve heykel malzemesi olarak yaygın kullanılmasına karşın mermerden farklı değerlendirilmiş ve ithalatının yapılmadığı düşünülmüştür.

Datça/Emecik arkeolojik kazılarında bulunan kireçtaşı figürinler M.Ö. 6. yy. Boyunca Akdeniz havzasında yaygın olan Kıbrıs tipi olarak tanımlanmıştır. Emecik'te bu tip figürinler çok sayıda ele geçtiğinde ham madde kaynağının belirlenmesi önemli bir problemdir.

Emecik figürinleri bazı major, eser elementler ve nadir toprak elementleri derişimleri açısından incelenmiş ve sonuçlar Emecik civarındaki bir taş ocağından alınan örneklerin bileşimi ile karşılaştırılmıştır. Analizlerde indüktif eşleşmiş plazma - optik emisyon spektrometrisi (ICP-OES) ve indüktif eşleşmiş plazma - kütle spektrometrisi (ICP-OES). Kullanılan yöntemin etkinliği ve doğruluğu standart referans madde ile kontrol edildi.

Anahtar Kelimeler: indüktif eşli plazma – kütle spektrometrisi, kireçtaşı, hammadde kaynağı, Kıbrıs figürinleri, nadir toprak elementleri.

To the memory of Savaş...

ACKNOWLEDGEMENT

I would like to express my deep appreciation to my supervisor Prof. Dr. O. Yavuz Ataman especially for his encouragement to study with his group in Chemistry Department, METU and for his guidance, understanding and friendship throughout this study. I am deeply grateful to Prof. Dr. Şahinde Demirci for her encouragement and contribution during the study.

I thank to Prof. Dr. Numan Tuna for offering me the subject of the study, selecting the figurine samples, suggesting the quarry and his guidance; to İlham Sakarya and Nadire Atıcı for their help for sampling. I thank to Assist. Prof. Dr. Uwe Müller, Prof. Dr. Elvan Yılmaz, Assist. Prof. Dr. Osman Yılmaz, Bülent Kızılduman, Eastern Mediterranean University for providing the geological samples from Cyprus. I would like to thank Prof. Dr. İbrahim Gündiler, New Mexico Bureau of Mines for providing the standard reference material NCS DC 73306.

I would like to thank for Prof. Dr. Asuman G. Türkmenoğlu for thin-section and XRD analyses of samples and for her guidance.

My special thanks to Sezgin Bakırdere for his endless assistance during my work especially regarding the instrumental analyses and for his invaluable support. I would like to thank all my friends in Atomic and Molecular Analysis Research Group for their friendship and kind support.

I also thank the examining committee members for their valuable contributions to my thesis.

Finally, I am appreciated to my mother, father and sister for their love and logical supports since the very beginning.

TABLE OF CONTENTS

PLAGIARISM.....	iii
ABSTRACT.....	iv
ÖZ.....	vi
ACNOWLEDGEMENTS.....	ix
TABLE OF CONTENTS.....	x
LIST OF TABLES	xii
LIST OF FIGURES.....	xiii
CHAPTERS	
1. INTRODUCTION.....	1
1.1. Limestone.....	2
1.1.1. Diagenesis of Limestone.....	3
1.1.2. Classification of Limestone.....	4
1.1.3. Physical Properties of Limestone.....	5
1.1.4. Chemical Properties of Limestone.....	7
1.2. Limestone Figurines.....	7
1.2.1. Cypriot Type Figurines.....	8
1.2.2. Emecik Figurines.....	11
1.2.3. Datça/Emecik Sarı Liman Excavations.....	14
1.3. Provenance Studies of Limestone.....	15
1.4. Provenance Studies of Figurines.....	23
1.5. Aim of the Study.....	25
2. EXPERIMENTAL.....	26
2.1. Chemical and Reagents.....	26
2.1.1. Water and Acids.....	26
2.1.2. Standard Solutions.....	26

2.2. Instrumentation and Apparatus.....	27
2.2.1. ICP – OES.....	27
2.2.2. ICP –MS.....	28
2.2.3. Microwave Dissolution System.....	29
2.3. Samples.....	30
2.3.1. Emecik Figurines.....	30
2.3.2. Geological Samples from Datça Peninsula.....	33
2.3.3. Geological Samples from Cyprus.....	35
2.4. Procedures.....	36
2.4.1. Microwave Assisted Dissolution.....	36
2.4.2. Dissolution by Fusion.....	37
2.5. Quantative Analysis.....	38
2.5.1. ICP – OES.....	38
2.5.2. ICP – MS.....	38
2.6. Thin-section Analysis.....	39
2.7. X-ray Diffraction Analysis.....	40
3. RESULTS AND DISCUSSION.....	42
3.1. Optimization of ICP-OES Conditions.....	42
3.2. Evaluating of Different Dissolution Procedures.....	42
3.3. Results of Analysis of Reference Materails.....	42
3.4. Results of Analysis of Figurines and Geological Samples.....	45
3.5. Results of Thin-section and XRD Analyses.....	47
3.6. REE Patterns and M-bird-grams of Figurines and Geological Samples.....	47
3.7. Element Ratios and Bianary Diagrams of Figurines and Geological Samples.....	52
4. CONCLUSION.....	55
REFERENCES.....	57

LIST OF TABLES

Table 2.1. Acids used in all experiments.....	26
Table 2.2. Standard solutions used in experiments.....	27
Table 2.3. Plasma conditions for ICP-OES, Leeman DRE.....	28
Table 2.4. ICP-MS, Thermo X series 2 plasma parameters.....	29
Table 2.5. Names and brief descriptions of samples.....	30
Table 2.6. Names and descriptions of geological samples.....	36
Table 2.7. Chosen wavelengths in ICP-OES, Leeman DRE.....	38
Table 3.1. Results for NIST 1d Argillaceous, Limestone.....	43
Table 3.2. Results for IGS 40.....	43
Table 3.3. Results for NCS DC 73306.....	44
Table 3.4. Results for figurines and geological samples with ICP-OES	45
Table 3.5. Results for figurines and geological samples with ICP – MS.....	46
Table 3.6. Values of REE, Ba and Sr in C1 chondrite.....	47
Table 3.7. TREE, LREE fractionations, Eu/Ce ratio and Ce anomalies of figurine and quarry samples.....	52

LIST OF FIGURES

Figure 1.1. Calcite mineral.....	3
Figure 1.2. Aragonite mineral.....	3
Figure 1.3. Dunham's classification for carbonate rocks.....	5
Figure 1.4. Thin section photomicrographs of oolitic limestone.....	6
Figure 1.5. Thin section photomicrographs of limestone with fossil fragments.....	6
Figure 1.6. Map of Mediterranean basin.....	9
Figure 1.7. Cypriot type lion figurine.....	10
Figure 1.8. Cypriot type figurine.....	10
Figure 1.9. Cypriot type figurine.....	10
Figure 1.10. Kouros figurine from Emecik.....	13
Figure 1.11. Head fragment of kouros from Emecik.....	13
Figure 1.12. Praying (priest ?)-offering figurine from Emecik.....	14
Figure 1.13. Lion figurine from Emecik.....	14
Figure 1.14. IUPAC Periodic Table.....	19
Figure 2.1. Plan of the Emecik excavation.....	32
Figure 2.2. Map of Datça peninsula, Tectonic units MTA 1997.....	33
Figure 2.3. Geological map of Datça peninsula, MTA 1997 1:100.000.....	33
Figure 2.4. Geological map of Cyprus.....	35
Figure 2.5. Microwave heating program.....	37
Figure 2.6. Thin-section photomicrograph of EMUT 18V, PPL, objective x4.....	40
Figure 2.7. Thin-section photomicrograph of EMUT 18V, XPL, objective x4.....	40
Figure 2.8. Thin-section photomicrograph of sample CD, PPL, objective x4.....	40
Figure 2.9. Thin-section photomicrograph of sample CD, XPL, objective x4.....	40
Figure 2.10. XRD trace of EMUT 18V.....	41
Figure 2.11. XRD trace of CD.....	41
Figure 3.1. REE patterns of Emecik figurines, EMLT16A11-a, 16A11-b, 16.148, 16.152 and 2.17.....	48

Figure 3.2. REE patterns of Emecik figurines, EMUT18V, EMLT10.26 and 16.151.....	48
Figure 3.3. REE patterns of Emecik figurines, EMLT28B.3, 9.21 and 18.4.....	49
Figure 3.4. REE patterns of the figurine EMLT4.65, stone sample EMLT4 and the geological sample CD.....	49
Figure 3.5. M-bird-grams of Emecik figurines, EMLT16A11-a, 16A11-b, 16.148, 16.152.....	50
Figure 3.6. M-bird-grams of Emecik figurines, EMLTU18V, EMLT2.17, 10.26 and 16.151.....	50
Figure 3.7. M-bird-grams of Emecik figurines, EMLT28B.3, 9.21 and 18.4.....	51
Figure 3.8. M-bird-grams of the figurine EMLT4.65, the stone sample EMLT4 and the geological sample CD.....	51
Figure 3.9. Ba vs Sr binary diagram of figurines.....	53
Figure 3.10. Ba vs Fe ₂ O ₃ binary diagram of figurines.....	54

CHAPTER 1

INTRODUCTION

Provenance studies, determination the source of the archaeological materials, play an important role in the understanding and reconstruction of trade connections, and social, political and religious relationships of ancient societies. Since 1960's, instrumental methods of analytical chemistry have been used for archaeological provenance studies of various artifacts, such as lithic, ceramic, glass and metal, although obsidian was the first and most widely analyzed material [1]. However, there are only a few provenance studies on limestone materials, since, unlike marble, limestone is generally considered to be local [2, 3, 4]. A great number of figurines from Emecik (Datça), which are the subjects of this study, resemble the type classified as *Cypriot* and bring up the arguments on the origins of these type of figurines which have been found all around the Mediterranean.

This study involves raw material properties and possible provenance of these figurines. Thesis presentation consists of four chapters:

First Chapter is the Introduction to limestone, archaeological limestone figurines, previous limestone provenance studies on limestone both archaeometric and geological and Emecik archaeological excavations.

Second Chapter is about the experimental part of the study, explains the sample collecting, procedures, e.g. instrumentation, apparatus, dissolution of samples and quantitative analysis.

Third Chapter is the Results and Discussions

Fourth Chapter is the Conclusion.

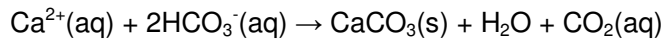
1.1. Limestone

Emecik figurines are supposed to be made of *limestone* [5]. Limestone is essentially composed of calcium carbonate mineral, CaCO_3 . It is one of the most common species of the chemically precipitated sedimentary rocks [6].

1.1.1. Diagenesis of Limestone

Although the calcium carbonate mineral may be precipitated directly from seawater, limestone is the result of organic precipitation. Many living organisms extract CaCO_3 from water to build hard protected shells. After the death of organisms, the hard calcareous parts accumulate on the sea floor. When marine life is abundant, shells of great thickness and other hard parts may build up, which, when consolidated, become limestone.

Precipitation of calcium carbonate can be shown by the following reaction equation [7] :



After the precipitation and deposition of calcium carbonate, it hardens into limestone through the growth of crystals and has two principal forms, *calcite* and *aragonite*. Deposition of calcite is of either high-magnesium or low-magnesium calcite [8]. Aragonite is a less stable form and changes to calcite in time. If the MgCO_3 content of calcite is greater than 4 % by weight, it is called high magnesium calcite, while if it is less than 4 % the calcite is called low magnesium calcite. High-magnesium calcite is more soluble in water than low-magnesium calcite, eventually, in time this mineral is converted into low-magnesium calcite [8]. The appearances of calcite and aragonite minerals are given in Figure 1.1. and 1.2. respectively.



Figure 1.1. Calcite mineral



Figure 1.2. Aragonite mineral

On the other hand, dolostone, quite similar to limestone, is also a sedimentary carbonate rock composed largely or entirely of the mineral *dolomite* $\text{CaMg}(\text{CO}_3)_2$ [9]. Limestone is recognized by the bubbly evolution of CO_2 gas when a few drops of dilute HCl are dropped on it, however dolomite does not react visibly with dilute HCl unless the mineral is powdered.

Carbonate rocks are normally quite free of impurities, which total less than 5 % of an average limestone and consist of clay minerals and fine-grained quartz [9]. Impurities could be introduced at any stage of deposition of the sediment [10], such as the transfer of water-borne suspended materials, mainly clay and silt, and dissolved elements, Mg, Si, F, Pb, Fe and other heavy metals, into faults, then these elements may have migrated from fault into the deposition through cracks and pores in limestone.

Diagenesis is the conversion of sediments into rock by organic, physical and chemical processes [10]. Six main processes have been identified for limestone: *microbial micritization*, *cementation*, *neomorphism*, *dissolution*, *compaction* and *dolomitization* [11]:

In *Microbial micritization*, the bore-holes made by organism in carbonate deposits become filled with a calcium carbonate structure called *micrite*.

Cementation results from the passage of water, which is super-saturated with respect to calcite, through porous limestone deposits, leading to the growth of calcite crystals in pores and because of that binding together the components of the deposit.

Neomorphism involves recrystallisation. Aragonite progressively recrystallises over time to produce very low-magnesium calcite. Calcite recrystallises into larger crystallites, so the magnesium in high-magnesium calcite slowly dissolves and leave low-magnesium deposits.

Dissolution generally occurs when unsaturated ground waters flow through deposits.

Compaction occurs during the burial process and is a combination of physical effects, such as dissolution/recrystallisation under high pressure.

Dolomitization results in the formation of the double carbonate $\text{CaCO}_3 \cdot \text{MgCO}_3$. The mechanisms of dolomitization are not well understood, but involve passage of seawater through the pores of limestone over long periods [10]. The dissolved magnesium is able to replace calcium ions in the crystal lattice, because dolomite is more stable than calcite.

1.1.2. Classification of Limestone

Limestone takes many forms and according to these forms it is classified as *bioparites*, *micrites*, *reef limestones*, *algal limestones*, *travertine* and *tufa* [10]. However, there are also many other ways of classifying limestone, which have been developed to describe the nature of the deposit. These classifications may be based on:

the average grain size [12],

micro-structure [11],

texture [11],

principal impurities, e.g. carbonaceous, ferruginous, argillaceous, or clayey, phosphatic [11] *carbonate content*, e.g. ultra-high calcium, high-calcium, high purity carbonate, calcitic, magnesian, dolomitic, high magnesium dolomite.

As an example, Durham classification for carbonate rocks based on texture and grain size is given in Fig.1.3. However, in study this classification is not followed, only the petrographical identification is given.






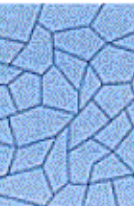
Mudstone	Wackestone	Packstone	Grainstone	Boundstone	Crystalline		
							
Less than 10% grains	More than 10% grains	Grain-supported	Lacks mud and is grain-supported	Original components were bound together	Depositional texture not recognizable		
Mud-supported							
Contains mud, clay and fine silt-size carbonate							
Original components were not bound together							
Depositional texture recognizable							

Fig.1.3. Dunham classification for carbonate rocks [13]

1.1.3. Physical Properties of Limestone

The color of limestone usually reflects the levels and the nature of the impurities present [10]. White deposits are generally of high purity; various shades of grey and dark hues indicate carbonaceous material or iron sulfide; yellow, cream and red hues are indicative of iron and manganese [10].

The texture of limestone varies widely. All limestones are crystalline with grain sizes ranging from less than 4 μm to about 1000 μm . The distribution of grain sizes affects the texture and ranges from mudstone to grainstone [10].

Crystal structures of calcite and aragonite are rhombic or hexagonal, while dolomite is trigonal [14]. At a wavelength of 590 nm calcite has ordinary and extraordinary refractive indices of 1.658 and 1.486, respectively [14].

The specific gravities of the crystalline forms of calcium carbonate and dolomite at 20 °C are calcite 2.71, aragonite 2.93 and dolomite 2.87 [14].

The porosity of limestones is generally in the range 0.1 to 30 % and of dolostones 1 to 10% by volume [10].

The hardness of limestones generally lies in the range 2 to 4 Mohs [10].

The bulk density of a limestone with an apparent density of 2.7 g/cm^3 is 1.40 - 1.45 g/cm^3 [10].

Thin section photomicrographs of oolitic limestone and limestone with fossil fragments are given in Fig.1.4 and Fig.1.5.

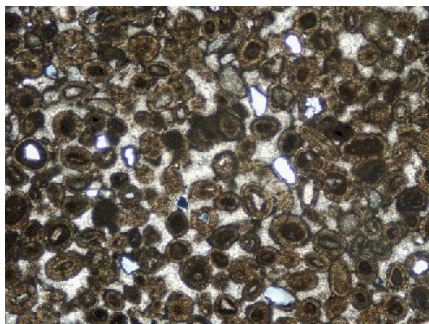


Fig.1.4 Limestone oolitic,
field of view 4.5 mm PL [OESIS]

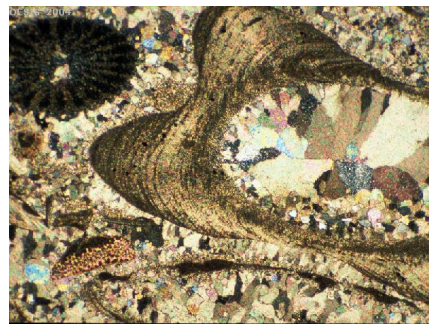
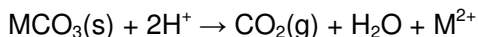


Fig.1.5. Limestone with fossil fragments,
field of view 3.5 mm PL [OESIS]

1.1.4. Chemical Properties of Limestone

The solubility of aragonite has is 0.0015 g/L, and of calcite is 0.0014 g/L under ambient conditions and calcite is metastable with respect to dolomite [14].

When limestone reacts with acids, CO₂ is released



where M shows Ca²⁺ or Mg²⁺.

It also releases CO₂ on heating and form calcium oxide, usually known as burnt or quick lime

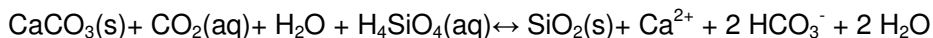


Calcium carbonate reacts with water that is saturated with carbon dioxide and forms the soluble calcium bicarbonate [14]



This is the reaction that is the reason of the formation of caverns and the temporary hard water. Limestone is alkaline with the pH values of 8 to 9 depending on the temperature.

Silicification process most likely occurs at low pH, low temperature environments in this process accumulation of silica in pores takes place [10]. Silification reaction can be shown as follow:



1.2. Limestone Figurines

People around the Mediterranean and in Anatolia used limestone since Neolithic times both as a building material and as a raw material for sculpture. Especially in Egypt, Cyprus and Levant limestone artwork expanded more than marble artwork,

because besides the unavailability of marble in this geography, the limestone can be more easily carved, shaped and transported than marble [10]. Figurines made of limestone were found even in Neolithic sites of Çatalhöyük [15], Göbekli Tepe [16] and Nevali Çori [16]. Limestone figurines were popular in Aegean region in Archaic Period, 6th century BC, as votive objects. They have been generally found in sanctuaries [17].

1.2.1. Cypriot Type Figurines

The type of limestone figurines classified as Cypriot, was popular during the Orientalizing (last quarter of 7th century B.C.) and Archaic periods (middle of 6th century B.C.) [17, 18]. Figurines were found not only in all sites in the Island, but also in various sites in Aegean region, Egypt, and Syro-Palestinian sanctuaries. Map of Mediterranean basin is given in Figure 1.6.

The size of the figurines are generally 10-20 cm; however larger pieces of 40-70 cm, have also been found [18]. Pictures of some figurines found in Rhodes are given in Fig.1.7., 1.8., and 1.9.

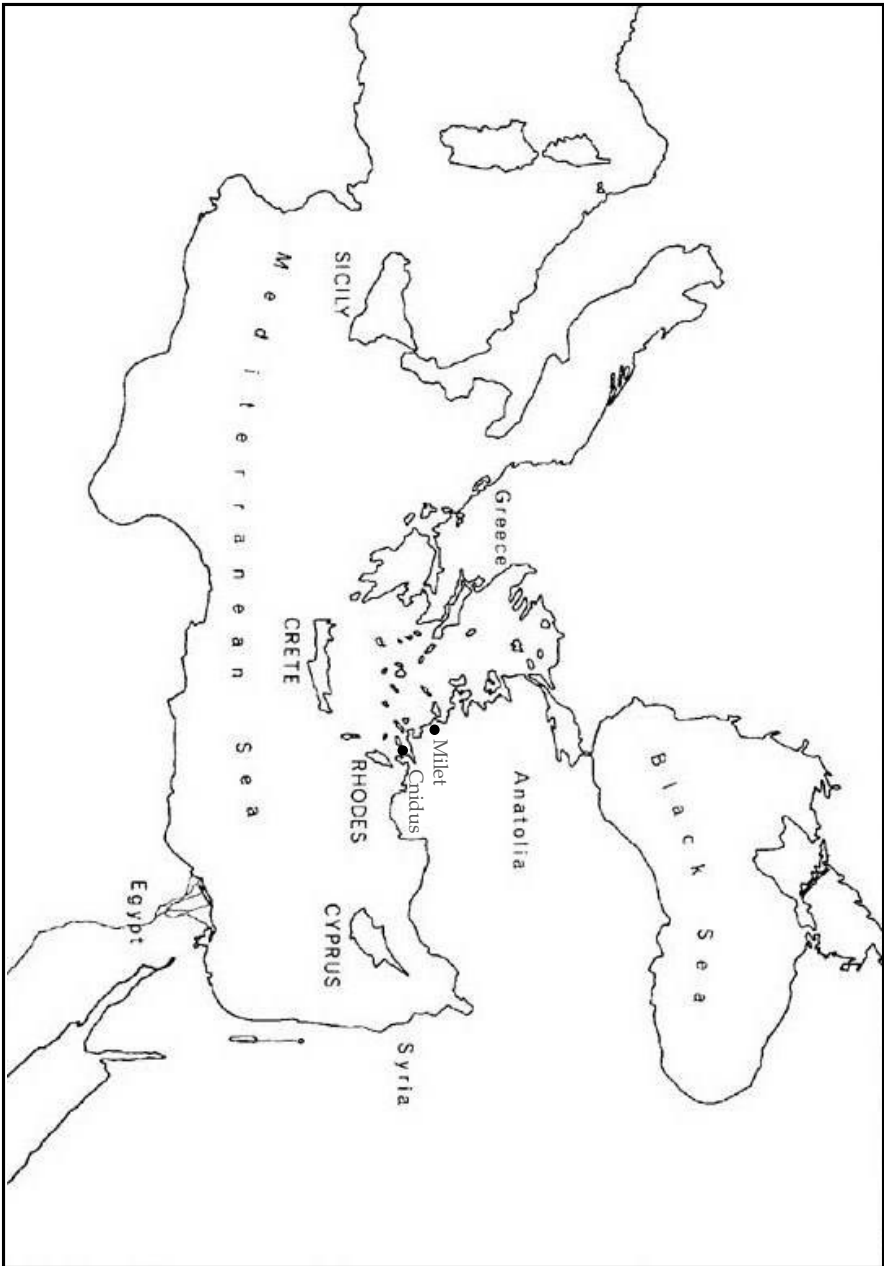


Fig. 1.6. Map of Mediterranean basin



Fig.1.7.Cypriot type lion figurine [18]

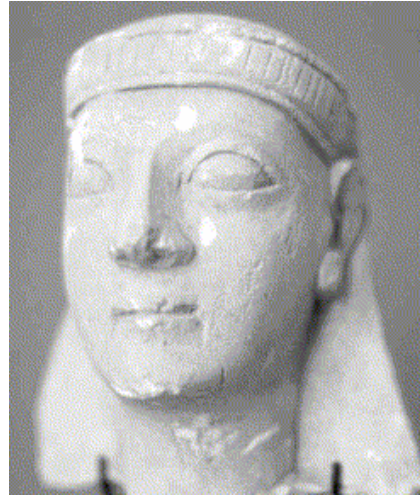


Fig.1.8. Cypriot type figurine [18]

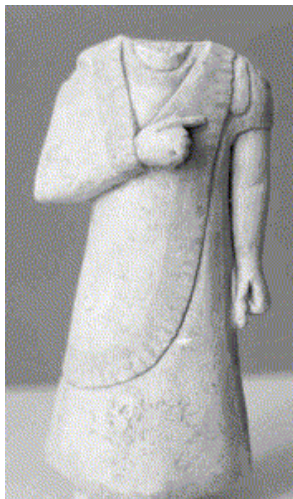


Fig.1.9. Cypriot type figurine [18]

The extended distribution of the figurines and the varieties in their styles raised the questions on the origins of them and this has been an argumentative issue for archaeologists. The period when the development in the monumental Greek sculpture took place corresponds to the time that the early figurines are dated and some archaeologists studying especially on Greek sculptural art even considers the figurines as the miniature Greek kouroi, male statues [19]. The initiation of this art in

Greece has Egyptian origins, since during the middle of 7th century B.C. Greeks were closely in contact with Egyptians, especially when according to Herodotus Greek military forces were in Egypt in Psammetichos I time, however, it developed its own Greek style within time [20].

These figurines range from purely Cypriote to a mix styled that includes Ionian, Aegean, and Egyptian elements [21]. Scholars have tried to group the figurines according to their styles as Aegean [21] or mixed Cypro - Aegean [17] and this kind of distinctions are generally accepted. However, the places of production are a more controversial issue. Some of the researches defend that there were also local ateliers other than Cyprus [20]; but the others advocate a popular assumption which says the whole corpus was of Cypriot type and they were produced by Cypriots either in Cyprus, in other local ateliers or by traveling craftsmen [17, 18, 20, 21, 22]. The latter theory explains the variations in style and iconography as they were made in Cyprus for the desire of different Aegean markets, although the mix styled figurines have been found in Cyprus rarely [20]. This is in contrast with contemporary Cypriot terracotta figurines that were also exported but avoid foreign elements [21].

Generally, instead of searching for other places of production, the provenance of the limestone of which the figurines were made has been considered to be as the evidence of the Cypriot origins [17, 18, 21, 23]. Because of this, some researchers even believe that the figurines were carved outside of Cyprus by Cypriot craftsmen using limestone pieces brought with them since limestone could be easily transported [17]. There are also some theories on the transportation of limestone mention that the limestone was used as the balance stone in ships and later the figurines were carved out of this balancing stone [20]. A few researches endorse these ideas on Cypriot origin of figurines; however they have also mentioned about a possible atelier in Cnidus [20, 23].

1.2.2. Emecik Figurines

The figurines that have been found in numerous amounts in Emecik are of a style, which is definitely different from what is defined as Cypriot [24, 25, 28]. The types of Emecik figurines, the distribution of the similar types in Mediterranean region and

possible dating were studied in a recent work by Berges [20]. However, this work include only a small part of the all findings; besides the stratigraphy and the context where the figurines are found are not mentioned in this work, for the dating they are evaluated stylistically and compared with the other figurines previously found around the Mediterranean. Some of these figurines are now in museums and some are in the storeroom of the Emecik excavation complex.

Although their original places or situations are not known since they are mostly from filling debris of south terrace wall, they are dated before the time when this wall was constructed e.g. before the last quarter of 6th century B.C. [24, 25, 26].

The limestone was described in Berges' work as very white, although varieties such as light grey, which are somehow harder, or brownish, and soft, even too soft to be carved for bigger statutes [20]. They were made by a sharp chisel and cut marks can be seen. Some of these figurines also have inscriptions on them and some bears traces of paintings.

The types of Emecik figurines are given below [20],

Kouroi, male figurines, fragments including head, body, leg and base, picture of a kouros is given in Fig.1.10 and 1.11.

Praying (priest ?) and offering figurines, fragments including head, body, picture of this type of figurine is given Fig.1.12.

Musicians, including flute or lyre playing

Male figures sitting on a throne, resembles the type were found in Didyma, showing a man having a self-confidence, probably representation a local person

Goddess with a ram sitting on a throne, representing which god is not clear, could be Zeus Ammon or Baal Hamon. This type may have connections to Egyptian or Near East iconography; beside it could be also related with Apollon cult because of the ram figure. Same type of figurines was found in Milet, Samos, Ialysos, Lindos in Rhodes, and Salamis in Cyprus .

Goddess holding (catching?) a lion, probably representation of a goddess, has iconographical connection to Near East, North Syria and also to East Greek. Same type of figurines was found in Samos, Lindos, Kamiros in Rhodes, Salamis in Cyprus, and Naucratis in Egypt.

Lion figurines, representing in sitting position, picture of a lion figurine is given in Fig.1.13. They are related to Apollon cult and have Egypt and North Syria origins. Although they have found sporadically in Cyprus and Naucratis, the main distribution of them with in the Dodecanese region, Chios, Samos, Milet, Lindos, Kamiros, Ialysos.



Fig.1.10. Kouros figurine from Emecik [28]



Fig.1.11. Head fragment of kouros from Emecik [28]



Fig.1.12. Praying (priest ?)-offering figurine from Emecik [TAÇDAM archive]



Fig.1.13. Lion figurine from Emecik [28]

Falcon figurines, one has an inscription on it and it is probably related to an Oracle, therefore it can be assumed that there was an Oracle in Emecik sanctuary. Same type has been found in Samos, Ialysos, Kamiros and Lindos.

Bull and ram figurines related to Apollon cult have also been found in Emecik, while terracotta figurines of bull type have been obtained numerously in Emecik.

1.2.3. Datça/Emecik Sarı Liman Excavations

The Archaic sanctuary in Emecik is located 15 km east of Old Knidos, Burgaz, in Datça peninsula from where Rhodes is approximately 18 km away. The area is in the mountain region, Kocadağ Mountain is in the north and southern part rises over Sarı Liman Bay, however it is not clear that what the coast line was in ancient times [20]. Because of these topographical features, the area was a proper place to be used as a harbor. The surface of the area is about 100 m and 80 m, and 32-45 m above the sea level. [27]. Two aerial photographs and the plan of the site are given at Figures A.2 and A.3.

The site has been excavated since 1998 by the supervision of Tuna [28]. The sanctuary is situated on a terrace; the southern wall bordering the sanctuary is by the Datça-Marmaris highway. The excavations are focused on upper terrace, Hellenistic structure and lower Terrace [28]. An Early Byzantine Church was unearthed in 1998 excavation period on upper terrace. The length of church is 20.3 m, width is 14 m and was built mainly with reused materials [24].

The other preserved monumental structure is of Hellenistic and it is understood to be a Doric temple, which has a peripteral plan with a krepidoma of 6 by 11 column stylobate and three krepis [28].

The lower terrace, considered as to be the central area during the Archaic Period, has given important stratigraphical information for the development of sanctuary. The south wall of sanctuary bordered the lower terrace. The figurines that were sampled for this study have been found in that area together with other imported votive objects, such as terracotta figurines. All these objects were found in filling layers of either artificial or natural. Therefore it is impossible to follow a regular chronology and stratigraphy. Based on these findings, such as votive figurines with ram, bull or lion representation, it is indicated that Emecik sanctuary was related to Apollon [21].

According to the results of excavations the sanctuary was abandoned after Late Archaic Period (6th century B.C.) by the 4th century on cultic activities revived but in local sense until Late Classical Period (4th century B.C.) and as the church at upper terrace shows that it was used through Byzantine times. In the northwest of sanctuary, there is also a cult cave and a spring that defined the location of sanctuary [24].

1.3. Provenance Studies of Limestone

As the literature showed many researches and publications have been made for provenance of various objects and materials. These works are especially concentrated on archaeometric investigations of marble, obsidian and ceramic findings and geological searches of sediments.

Still, there are not many provenance studies on limestone. The reason of this could be the theory that advocates apart from some valuable stone material, such as marble, the trade of limestone was not made in ancient times, the limestone used as building material or to make sculpture and other small objects was came from a local quarry. Besides the, these studies on limestone are based on the petrographic, isotope, and X-ray powder diffraction analysis and determination of major, minor and trace elements, establishment of the appropriate elements for provenance in both man made samples and natural sources and interpretation of the results in the terms of statistical probabilities.

An extensive study, Brookhaven Limestone Database Project, is carried on by the International Center of Medieval Art on limestone sculptures and monument especially within France [4, 29, 30, 31]. In this project, Neutron Activation Analysis (NAA) is used in compositional characterization of limestone and the elements for discriminate the groups of samples are selected, e.g. rare earth elements, alkali and transition elements [4, 31]. Concentration values of the elements then are evaluated by multivariate statistics [4, 29].

De Vito et al. studied on limestones used for two monuments dated to 4th – 3rd centuries B.C. and 1st century B.C. – 1st century AD., in Italy and limestone samples as the possible geological raw materials [2]. In this work Atomic Absorption Spectrometry, AAS, isotopic analyses were used for the determination of major, minor and trace elements, of totally 12 elements; C and O isotopic compositions and microscopy for petrographic characterization of the samples were included. Na, Mn, Fe and Sr were selected because of their significance in carbonate sedimentation and diagenesis; Li, K and Rb were selected since they are considered diagnostic in carbonate sedimentation; Ni, Co, Zn and Cu, since they are widely used to obtain paleo-environmental information. Ternary plots for Li-Rb-Pb and Pb-Co-Ni are shown and the authors concluded that Pb-Co-Ni could not discriminate between samples.

Marinoni et al. studied black limestone samples used in architecture obtained from three quarries in Italy in order to provide a characterization and determination of provenance [3]. Samples were separated into organic and inorganic fractions. Inorganic fractions were characterized in terms of textural features by optical

microscopy, mineralogical features by XRD analysis, chemical compositions by AAS, and C and O isotopic ratios. Fe, Mn, Cd, Co, Cu, Zn and Sr, which substitute Ca in calcite-like structures, were determined as well as Na. Binary diagrams, Fe/Mn, Co/Zn, Sr/Zn and Cd/Na, were used to mark compositional differences.

In another work by Bello and Matin [32], limestone material, which was used in the construction of Cathedral of Seville, Spain, and samples from six different quarries, were examined. Flame Emission Spectroscopy (FES) and AAS were used to determine fourteen trace elements, Rb, Cs, Sr, Ti, Cr, Mo, Mn, Ni, Cu, Zn, Cd, Sn, Pb, Sb. SiO_2/CaO ratio characterized eight different groups from Cathedral stones. Two groups among them were chosen to identify their geological sources by enrichment diagrams of trace elements (ETDE). ETDE results, confirmed by cluster analyses, were found useful for provenance determination.

Harell studied on twenty-three ancient Egyptian limestone quarries in the Nile Valley to obtain provenance indicators that differs each [33]. Si, Al, Ca, Mg, Na, K, Fe, Ti and P were determined using XRF method and examined using thin-section petrography in totally twenty-eight samples. According to the results, geological formations could be identified by petrography and XRF analyses. $\text{CaO}/[\text{CaO} + \text{MgO}]$ vs. $\text{SiO}_2/\text{Al}_2\text{O}_3$ plot were applicable to narrow the possibilities of two or three formations and then petrographic parameters will identified the most likely source within the quarries.

Another study for obtaining provenance indicators of limestone in Greece was done by Wenner and Herz [34]. The authors worked on samples from monuments and quarries in two regions and isotope analysis as well as petrographic observations appeared to be useful for discriminating the different sources and determination the provenance of the archaeological samples.

Moreover there are geological researches on limestone and other sediments for provenance and diagenesis of the rocks especially based on their rare earth elements (REE) compositions.

Rare Earth Elements

In the periodic table f-block elements are composed two series of metal: the lanthanoids, the 14 elements that follow La, and actinoids, the 14 elements that follow Ac [52]. Periodic table is given in Fig.1.14. Sc, Y, La and lanthanoids are together called the rare earth elements (REE) [52, 53, 54], although the true rare earths are the elements occurring in periodic table between 58-71 [54]. In the elements in this part of the periodic table, 58-71, as the charge on the nucleus increases, the balancing electron fill in the inner incomplete 4f subshells [54]. This subshell can hold 14 electrons and 4f electrons are well screened by the completed 5s5p subshells, they play almost no part in the valency forces, although they play very important role in some physical properties such as magnetism and spectra [54]. Outer shell electrons screened 4f electrons are held tightly by the nucleus and atomic radii do not increase [55]. In fact, in the series of elements in which 4f subshell is filled, atomic radii decrease and this phenomenon is called lanthanoids contraction [55]. All the elements between 58-71 have three electrons in their valency shells in aqueous media and because the outermost electrons of an atom are responsible for most physical and chemical properties, these elements closely resemble each other in this media. The fact that IIIA group in periodic table has elements, which also have 3 electrons in the valency shells, makes these elements closely resemble the elements between 58-71, and moreover Y and La are almost always found associated with these true rare earths [54]. For these reason they are also frequently referred as rare earth elements [54]. The descriptive classification of rare earths is established according to their atomic numbers: light rare earth elements (LREE) comprise La to Eu, middle rare earth elements (MLEE) Sm to Ho, and heavy rare earth elements (HREE) Gd to Lu [53]. Due to their electronic configuration they are stable in earth and used in most of the provenance studies [35, 36].

1																		2																		3																																																																																																																																																																																																																																																																																																																																																																																																																																																																																																																																																																																																																																																																																																																																																																																																																																																																																															
1 H Hydrogen 1.007 84(7)																		2 He Helium 4.002 602(2)																		3 Li Lithium 6.94(1)																		4 Be Beryllium 9.012 183(1)																		5 B Boron 10.81(1)																		6 C Carbon 12.010 7(8)																		7 N Nitrogen 14.006 4(1)																		8 O Oxygen 15.999 4(1)																		9 F Fluorine 18.998 403(1)																		10 Ne Neon 20.179 7(6)																																																																																																																																																																																																																																																																																																																																																																																																																																																																																																																																																																																																																																																																																																																																																																	
11 Na Sodium 22.989 769 28(2)																		12 Mg Magnesium 24.304 0(6)																		13 Al Aluminum 26.981 538 6(8)																		14 Si Silicon 28.085 5(8)																		15 P Phosphorus 30.973 762(2)																		16 S Sulfur 32.06(5)																		17 Cl Chlorine 35.45(2)																		18 Ar Argon 39.948 1(6)																																																																																																																																																																																																																																																																																																																																																																																																																																																																																																																																																																																																																																																																																																																																																																																																					
19 K Potassium 39.098 3(1)																		20 Ca Calcium 40.078 4(4)																		21 Sc Scandium 44.955 912(3)																		22 Ti Titanium 47.867 1(8)																		23 V Vanadium 50.941 5(1)																		24 Cr Chromium 51.996 1(6)																		25 Mn Manganese 54.938 044(3)																		26 Fe Iron 55.845 2(6)																		27 Co Cobalt 58.933 195(3)																		28 Ni Nickel 58.693 4(4)																		29 Cu Copper 63.546 3(8)																		30 Zn Zinc 65.38(4)																		31 Ga Gallium 69.723 1(3)																		32 Ge Germanium 72.630 0(8)																		33 As Arsenic 74.921 595(2)																		34 Se Selenium 78.96(3)																		35 Br Bromine 79.904 1(8)																		36 Kr Krypton 83.798(2)																																																																																																																																																																																																																																																																																																																																																																																																																																																																																																																																																																																																																	
37 Rb Rubidium 85.467 8(3)																		38 Sr Strontium 87.62(3)																		39 Y Yttrium 88.905 842(3)																		40 Zr Zirconium 91.224 0(8)																		41 Nb Niobium 92.906 38(3)																		42 Mo Molybdenum 95.94(2)																		43 Tc Technetium 98.906 254(3)																		44 Ru Ruthenium 101.07(2)																		45 Rh Rhodium 102.905 50(2)																		46 Pd Palladium 106.905 08(2)																		47 Ag Silver 107.868 2(4)																		48 Cd Cadmium 112.411 8(8)																		49 In Indium 114.818(1)																		50 Sn Tin 118.710(7)																		51 Sb Antimony 121.757(3)																		52 Te Tellurium 127.60(3)																		53 I Iodine 126.905 47(3)																		54 Xe Xenon 131.29(4)																		55 Cs Cesium 132.905 451 9(2)																		56 Ba Barium 137.327(7)																		57 La Lanthanum 138.904 877(7)																		58 Ce Cerium 140.116(1)																		59 Pr Praseodymium 140.907 68(2)																		60 Nd Neodymium 144.242(3)																		61 Pm Promethium [144]																		62 Sm Samarium 150.36(2)																		63 Eu Europium 151.964(1)																		64 Gd Gadolinium 157.25(3)																		65 Tb Terbium 158.925 36(2)																		66 Dy Dysprosium 162.50(3)																		67 Ho Holmium 164.930 32(2)																		68 Er Erbium 167.259(3)																		69 Tm Thulium 168.934 21(2)																		70 Yb Ytterbium 173.054(7)																		71 Lu Lutetium 174.967(1)																		72 Hf Hafnium 178.49(2)																		73 Ta Tantalum 180.947 88(2)																		74 W Tungsten 183.84(1)																		75 Re Rhenium 186.207(1)																		76 Os Osmium 190.23(3)																		77 Ir Iridium 192.222(3)																		78 Pt Platinum 195.084(3)																		79 Au Gold 196.966 569(4)																		80 Hg Mercury 200.59(2)																		81 Tl Thallium 204.38(3)(2)																		82 Pb Lead 207.2(1)																		83 Bi Bismuth 208.980 401(3)																		84 Po Polonium [209]																		85 At Astatine [210]																		86 Rn Radon [222 219.97(6)]																	
72 He																		73 Li																		74 Be																		75 B																		76 C																		77 N																		78 O																		79 F																		80 Ne																																																																																																																																																																																																																																																																																																																																																																																																																																																																																																																																																																																																																																																																																																																																																																																			
Fr																		Ra																		Ac																		Th																		Pa																		U																		Np																		Pu																		Am																		Cm																		Bk																		Cf																		Es																		Fm																		Md																		No																		Lr																		Hf																		Ta																		W																		Re																		Os																		Ir																		Pt																		Au																		Hg																		Tl																		Pb																		Bi																		Po																		At																		Rn																																																																																																																																																																																																																																																																																																																																																					
Fr																		Ra																		Ac																		Th																		Pa																		U																		Np																		Pu																		Am																		Cm																		Bk																		Cf																		Es																		Fm																		Md																		No																		Lr																		Hf																		Ta																		W																		Re																		Os																		Ir																		Pt																		Au																		Hg																		Tl																		Pb																		Bi																		Po																		At																		Rn																																																																																																																																																																																																																																																																																																																																																					



57 La Lanthanum 138.904 877(7)	58 Ce Cerium 140.116(1)	59 Pr Praseodymium 140.907 68(2)	60 Nd Neodymium 144.242(3)	61 Pm Promethium [144]	62 Sm Samarium 150.36(2)	63 Eu Europium 151.964(1)	64 Gd Gadolinium 157.25(3)	65 Tb Terbium 158.925 36(2)	66 Dy Dysprosium 162.50(3)	67 Ho Holmium 164.930 32(2)	68 Er Erbium 167.259(3)	69 Tm Thulium 168.934 21(2)	70 Yb Ytterbium 173.054(7)	71 Lu Lutetium 174.967(1)
89 Ac Actinium [227]	90 Th Thorium 232.037 7(4)	91 Pa Protactinium 231.036 89(2)	92 U Uranium 238.028 91(3)	93 Np Neptunium [237]	94 Pu Plutonium [244]	95 Am Americium [243]	96 Cm Curium [247]	97 Bk Berkelium [247]	98 Cf Californium [251]	99 Es Einsteinium [252]	100 Fm Fermium [257]	101 Md Mendelevium [258]	102 No Nobelium [259]	103 Lr Lawrencium [262]

Notes:
 - Numerical and textual are currently used alternative codings for numerical and textual.
 - IUPAC 2005 standard atomic weights (or mass relative atomic masses) are listed with uncertainties in the last figure in parentheses (e.g. 1.007 84(7)).
 - These values correspond to current best knowledge of the elements in related scientific sources. For elements that have no stable or assigned nuclei, the mass number of the nucleus with the longest confirmed half-life is listed between square brackets.
 - Elements with atomic numbers 112 and above have been reported but not fully substantiated.
 Copyright © 2007 IUPAC, the International Union of Pure and Applied Chemistry. For updates to this table, see <http://www.iupac-atomicweights.net>. This version is dated 30 March 2007.

Fig. 1.14. IUPAC Periodic table

Importance of REE Pattern

REE value of a sample could be found by its REE pattern. This pattern is a graph that shows normalized REE values versus atomic numbers in logarithmic scale. Normalized values are found by dividing the concentration of a REE in the sample to its value in either a meteoric stone, such as chondrite, upper crust or shale values and the value is shown with a * subscript such as Yb_{cn} . The REE pattern is related directly to the chemical composition of the stone. The constant relation of the REE pattern and the type of stone is a result of the atomic structure of REE.

This pattern is an important tool for understanding the geochemical processes and also to detect anomalous data that could be due to natural processes, anthropogenic contamination, in field or laboratory, or analytical error [43].

Some of these geological studies are given below:

Cullers worked on shales and limestones in Pueblo, Colorado, USA for the provenance, the redox conditions and the metamorphism of the rocks [37]. Major and some trace elements concentration including REE were determined using AAS and NAA. In order to realize which elements are incorporated into carbonate phase, samples were also treated with HCl to obtain acid insoluble residue, non-carbonate phase of the stone. According to plots of element oxides vs. % residue, CaO vs. % residue, SiO_2 , Al_2O_3 , Fe_2O_3 , MgO, Na_2O , K_2O , TiO and Sm, Eu, Tb, Yb, Lu, Ta, Sc, Th, Cr, Hf, Cs and Rb are incorporated into residue while La and Ce are held in silicate minerals included in the insoluble residue with a lesser amount exited in calcite and Sr, in contrast, included in the calcite. The Th/Co, Th/Sc, Th/Cr, La/Co, La/Sc, La/Cr, La/Lu ratios and Eu/Eu* that are characteristics of the provenance of terrigenous sedimentary rocks and Ce/Ce* that is used to interpret the redox conditions of the seawater at the time the REE were incorporated into marine sediment.

Another study on the provenance of playa sediments in India, REE, major and trace elements were determined using ICP-MS and XRF, mineralogical investigations were carried out using XRD [38]. The detrital-rich samples show enriched values of SiO_2 , Al_2O_3 , K_2O , TiO_2 , Fe_2O_3 , Zn, Rb, Cr, Ni, Ba and Zr. Similarly, the samples

containing calcite and dolomite have higher abundances of Cu, Sr, CaO, MgO. Meantime, Y and Th showed a strong positive correlation and Rb, Ba, TiO₂ show significant correlation with all REE and total REE (TREE). Zr influences only LREE while CaO, MgO and SR show negative correlations with REE. REE patterns, fractionation of LREE (La/Sm)_n, HREE (Gd/Yb)_n, TREE (La/Yb)_n and Eu anomaly indicated different groups.

Bellance et al. studied the REE distribution in limestone / marlstone couplet in Southern Alps for investigation REE sensitivity to environmental changes [39]. REE and As, Cd, Mo, Sb, Th, Y and U were determined by ICP – MS. TREE content of the limestone shows a strong negative correlations with CaO. Limestone exhibit seawater-like REE pattern and both Ce anomaly and La/Yb fall in the range of average seawater and these indicate calcite uptaking REE from seawater in which it is formed. The correlation between Eu anomaly and other major or trace elements is not apparent, therefore it could be concluded that no single mineral is responsible for the anomaly.

Bolhar et al. investigated the chemical characterization of metasomatic sediments in Greenland evaluating major elements, first transition elements (Sc, V, Cr, Co, Ni), high field strength elements (HFSE: Zr, Hf, Nb, Ta, Y), strongly lithophile elements (Th, U, Rb, Sr, Ba). In the study, REE contents were determined by ICP-OES and ICP-MS [40]. SiO₂/Al₂O₃ vs K₂O/Na₂O, Ni vs. Cr, Zr vs. Hf, Nb vs. Ta, Y/Ho vs. Nb/Ta, Th vs. U plots and for REE (La/Sm)_{cn}, (La/Yb)_{cn} and (Gd/Yb)_{cn} and Eu/Eu* values were interpreted for the lithological makeup of the source stone, post depositional element mobilization and subaerial weathering.

In addition, the studies by Igarashi was on the REE determination in limestone geological reference material Ls-1 by ICP-MS [41], by Ionov on trace element distribution including REE of calcite – dolomite carbonatites in South Africa in order to investigate the factors that affect the composition [42], by Halicz on the REE determination in fresh water and comparison of REE pattern of water with that of the associated rocks [43].

When these studies are considered it can be understood that limestone has some chemical characteristics that help to interpret the diagenesis of the rock. An ancient

rock that began as a sediment with average of 50% or more porosity may have less than 10% porosity today [8]. This required either introduction of calcium carbonate approximately equal to the original solid volume of the rock or a loss of one-half of the original volume of the rock by compaction. There is abundant evidence that most carbonate rocks have undergone relatively little compaction. Thus, introduction of calcium carbonate from an outside source is required. The source of this calcium carbonate and its means of transportation and deposition within the rock should be one of the main problems of limestone diagenesis.

The distinction between dolostone and limestone is one of the main issues of the carbonate rocks. Dolostone could be best described as the rock composed largely or entirely of mineral dolomite $\text{CaMg}(\text{CO}_3)_2$ [9]. Dolomite forms in two ways: the origin of dolomite on the surface of the earth and the origin of dolomite in sedimentary rocks [44]. In both cases, pre-existing CaCO_3 react with solutions, resulting in the formation of dolomite. In this reaction metastable CaCO_3 , which forms in place of stable dolomite, is changed into dolomite by diagenetic solutions, which generally abundant in Mg. Different amounts of dolomite are thus formed from a definite amount of CaCO_3 depending on the anion contents of the medium [44].

The amounts of most of the minor elements in limestones are extremely variable among the samples and the differences are due largely to liquid or solid inclusions among calcite or aragonite crystals rather than to structural or interstitial substitutions of the minor elements for calcium ions [9]. In the diagenetic process of limestone, a decrease in strontium contents of limestones with increasing age has been noted and this decrease results from conversion of aragonite to calcite [9]. Moreover, the distinction between aragonite and calcite appears in the contents of some other elements: in aragonitic shells the abundance of Mg and Mn decrease with time, Ba and Fe increase, in calcitic shells Mg decreases, however other elements remain unchanged [9].

Above mentioned studies show that while REE are related to silicates within the rock matrix like some other trace elements such as Ti, Al, K, Na, Ba and so on, within REE La and Ce are also related to the carbonate fraction of the rock matrix [37]. There are also other studies that relate the REE patterns of the water reflected underlying water-rock interactions [43].

Although limestone is not as homogenous as igneous rocks such as obsidian since it is a sedimentary rock, some chemical characteristics, especially REE contents, are found to be discriminating the provenance of the limestone [45, 46]. These could be summarized as follows:

Total REE concentration, beside the LREE and HREE fractionations, found by La_{cn}/Lu_{cn} , or La_{cn}/Yb_{cn} and La_{cn}/Sm_{cn} respectively, Th/Sc , Th/Cr and Eu/Ce , ratios, Eu anomaly, Eu/Eu^* and Ce anomaly, Ce/Ce^* are used to discriminate different types of stone [35, 36, 38]. Ce/Ce^* ratio, which is calculated as $3Ce_{cn}/(2La_{cn} + Nd_{cn})$ [47], helps to interpret the redox conditions of when REE incorporated into the matrix. If this ratio is in the range between 0.4-0.7, it indicates an oxidized environment. If it increases to 1.0, it indicates a reduced environment [38]. Ce anomalies are also classified as extremely negative if the ratio is 0.33 – 0.50, if it is 0.50 – 0.69 sediments show moderately negative and if it is 0.69-1.47 show weak or no Ce anomalies [42].

1.4. Provenance Studies Of Figurines

The generally accepted assumption is that most of the statuettes are of Cypriot origin, if not all. This assumption is insufficient to answer some important questions such as the wide distribution and more important the varieties in style. Although the figurines found outside of Cyprus are stylistically quite different from Cypriot figurines, distinguishing stylistic classes based on the locations where they are found is very difficult since they all bear mixing elements of North Syrian, Cypriot, and East Greek art. Besides, archaeologists faced the case that how it is possible if all the figurines were made in Cyprus the this mix style ones have been found only rarely in the Island. Then they have begun to work with other scientists of different disciplines in order to search for the provenance of the limestone, raw material. The aims of these studies were to locate different ateliers other than Cyprus or prove that they were actually made in Cyprus to be exported to Aegean markets. However, a limited number of provenance studies on this area have been done so far.

The researches include microscopic examinations with optical microscopy; chemical analysis X-ray Fluorescence spectrometry (XRF), Electron Paramagnetic Resonance spectrometry (EPR), of archaeological samples and/or geological samples taken from quarries.

These studies are given below:

Kourou, Karageorghis studied on some Cypriot type figurines found in Cyprus, other figurines found at Aegean sites, and compared the results with those of quarries in Cyprus, Samos, Rhodes, and Naucratis using optical microscopy and EPR [17]. As it could be expected the chemical composition of the Cypriot samples are in accordance with the Cypriot geological samples, while, with some exceptions, the figurines from Samos are also similar to the Cypriot samples. The figurine from Egypt is found to be made either by Samian or Egyptian limestone but not Cypriot. All of the figurines from Rhodes, with one exception are also in accordance with Cypriot samples. So they concluded that the figurines they were examined were made from Cypriot limestone.

The work by Polikreti, Maniatis et al. is the more systematic research using EPR [18]. They collected samples from quarries in Cyprus, Samos, Rhodes, and Naucratis thought to be the most probable production centers for figurines. A numbers of figurine samples from Samos, Rhodes, were taken. Two other statuettes found in Cyprus were also sampled in order to compare with these two groups of sample. According to their results, limestone samples from Rhodes and Naucratis are physically insufficient for carving, chemical composition of samples from Samos are not similar to those of statuettes examined, On the other hand, properties of all sampled statuettes were matched the limestone of a specific geological formation in Cyprus.

The recent work by Berges, includes also XRF analysis of ten fragments of figurines and a Doric column fragment from Emecik, seven fragments of figurines from Milet, besides the geological samples from Cyprus, from a crop between Kızlan and Emecik, and also from different places around Emecik [20].

According to the results the author concluded that the chemical composition of the figurines both from Emecik and Milet including the column fragment from Emecik do not show much variation, therefore the raw material of them should be from the same quarry [20]. According to the interpretations in this work, based on the concentration values of the elements, the composition of the geological samples from Datça peninsula, however, is completely different therefore, Datça could not be

the geological source. Meantime, the geological samples from Cyprus are in accordance with the figurines both from Emecik and Milet, though the variations are present because of the heterogeneity of the stone matrix. Then the author concluded that the figurines were made from the Cypriot limestone.

It is obvious that the above mentioned few studies are not sufficient to resolve the problem of the provenance of enormous amount of figurines all around the East Mediterranean; because, for a strict scientific evaluation, results obtained from chemical analysis should be considered and compared with statistics and a databank for each possible production place and each group of figurines should be established. But up to now it has not been done yet.

1.5. Aim of the Study

In order to determine the provenance of a group of Emecik figurines dated from late 7th century B.C. to 6th century B.C., establishing proper digestion and analysis methods for archaeological and geological samples by ICP-MS and ICP-OES, are the aim of this study. 13 figurines and geological samples from modern quarries in Alyaka, Datça and in Taşkent, Güngörköy, Değirmentepe, Cyprus were examined to reveal the chemical composition and REE patterns of the samples; Mg, Fe, Sr, Ba and La, Ce, Nd, Sm, Eu, Yb, Lu were determined and the results were statically evaluated.

CHAPTER 2

EXPERIMENTAL

2.1. Chemicals and Reagents

2.1.1. Water and Acids

Milli-Q 18 M Ω -cm (Water Assoc.) deionized water and the acids listed in Table 2.1 were used in all procedures.

Table 2.1. Acids used in all experiments.

Acid	Producer and properties
HF	Merck, extra pure, 40 % (w/w)
HCl	Merck, analysis grade, 36 % (w/w)
HNO ₃	Merck, analysis grade, 65 % (w/w)
Flux reagents	Producer and properties
LiBO ₂	Merck, spectromelt A 20
Li ₂ B ₄ O ₇	J.T. Baker, flux grade

2.1.2. Standard Solutions

Aqueous standard solutions used in experiments are shown in Table 2.2.

Table 2.2. Standard solutions used in experiments

Standard	Concentration	Producer
Mg	1000 mg Mg/ L (in dilute HNO ₃)	Merck
Fe	1000 mg Fe / L (in dilute HNO ₃)	Merck
Ba	1005 mg Ba / L (in dilute HCl)	Aldrich
Sr	1005 mg Sr/ L (in dilute HCl)	Aldrich
La	1000mg La / L (in dilute HNO ₃)	Ultra Scientific
Ce	999 mg Ce/ L (in dilute HNO ₃)	Inorganic Ventures
Nd	1000 mg Nd/ L (in dilute HNO ₃)	Ultra Scientific
Sm	1000 mg Sm/ L (in dilute HNO ₃)	Ultra Scientific
Eu	1000 mg Eu/ L (in dilute HNO ₃)	Ultra Scientific
Yb	1000 mg Yb/ L (in dilute HNO ₃)	Ultra Scientific
Lu	1000 mg Lu/ L (in dilute HNO ₃)	Ultra Scientific

The dissolution procedures developed were performed using certificated reference materials SRM 1d, Limestone, argillaceous sample produced by National Institute of Standards and Technology, NCS DC 73306, Rock Reference Material produced by China National Analysis Center and IGS 40, Bastnasite, rare earth ore produced by MBH Analytical Ltd.

Durapore Membrane Filter, with 0.45 µm pore size, manufactured by Millipore was used as filtering medium.

2.2. Instrumentation and Apparatus

2.2.1. Inductively Coupled Plasma–Optical Emission Spectrometry, ICP – OES

Leeman DRE ICP-OES instrument was used for the determination of Mg, Fe, Ba, Sr, concentration in figurine samples. The instrument employs a photomultiplier tube (PMT) as detector and allows the use of the facility of sequential multi-element analysis. An axial plasma torch was used. Burgener 17 2002 Meinhard type nebulizer was used in sample introduction system of ICP – OES. The operating parameters of the instrument throughout the study were given in Table 2.3.

Table 2.3. Plasma conditions for ICP – OES, Leeman DRE.

Rf Power	1.3 kW
Nebulizer Gas	50 Psi
Auxiliary Gas	0.5 LPM
Coolant Gas	18 LPM
Pump Rate	1.2 L/min

2.2.2. Inductively Coupled Plasma – Mass Spectrometry, ICP – MS

Thermo X SERIES 2 ICP – MS instrument was used for the determination of La, Ce, Nd, Sm, Eu, Yb and Lu. Instrument has quadrupole analyzer and Protective Ion Extraction and Infinity II ion optics, based upon a hexapole design with chicane ion deflector, provides the lowest background specification of quadrupole ICP-MS. The quadrupole analyzer is pumped by a novel split flow turbo pump backed by a single rotary. The instrument has the simultaneous analog/PC detector with real time multi-channel analyzer electronics.

ICP-MS is finding increasing acceptance in geochemical applications particularly for the determination of REE, which are easily determined by ICP-MS as they are at the middle to high portion of the mass range and have few interferences from polyatomic plasma species [49]. Cerium very readily forms an oxide and Ba, meantime is most prone to formation of doubly charge species, so these elements are used the study for monitoring the probability of oxide and doubly charged ions formation. In general the upper limits of 3% for CeO/Ce, and BaO/Ba are generally accepted [50, 51]. In this study CeO/Ce ratio was better than 0.5 % and BaO/Ba ratio was 0.5%, while spray chamber is kept at 3°C for avoiding oxidization of elements. All measurements were repeated three times.

The tune conditions of the ICP-MS are given Table 2.4.

Table 2.4. ICP – MS, Thermo X series 2 plasma parameters

Plasma

Extraction voltage	-82.0	Horizontal voltage	63
Lens 1 voltage	-200	Vertical voltage	619
Lens 2 voltage	-26.7	DA voltage	-30.6
Focus voltage	16.3	Cool L/minute	13.0
D 1 voltage	-43.1	Auxiliary L/mine	0.90
D 2 voltage	-166	Depth	40
Pole Bias voltage	0.3	Standard resolution amu	125
Hexapole Bias voltage	- 0.8	High resolution amu	125
Nebuliser L/min	0.83	Analogue Detector voltage	2050
Lens 3 voltage	-197.6	PC detector voltage	3249
Forward power voltage	1400	Sample uptake L/min	1 L/min

Mass spectrometer data acquisition

Measurement mode Peak hop

Sweeps 110

Acquisition time 27 seconds

2.2.3. Microwave Dissolution System

Milestone Ethos PLUS microwave dissolution system was used in the closed system dissolution procedures. The system has a maximum power of 1000 W, which is controlled by a temperature probe. Simultaneously, at most of 10 vessels made of polytetrafluoroethylene (PTFE) can be placed in heating chamber.

In this study PTFE vessels were used instead of glassware since acid mixtures including HF for the dissolution by microwave oven affects the glass. Stable Pt crucibles which contain 5% Au were used for the dissolution by fusion of the samples. All dilutions were performed using polypropylene volumetric flasks.

At the end of each working period, vessels were cleaned in 10 % HNO₃ by heating on a hot plate for about 30 min. The volumetric flasks were immersed in 10 % HNO₃ at least for a night. All vessels were rinsed using pure water before use.

2.3. Samples

2.3.1. Emecik Figurines

Figurines were found in the lower terrace except one, which was found in the upper terrace of sanctuary. All samples were obtained during 1999 – 2002 excavation sessions. The sampled figurines were excavated from 2 trenches in the lower Terrace: ST02-01-99 I 8B, the filling debris where the votive figurines were found to be abundantly and ST00-99 K 8C, the filling debris of terrace wall and one from upper terrace ST00 d 8A.18.V, northeast of the Byzantine Church where a floor consisting of big conglomerate blocks was unearthed. The locations of these trenches are marked in the plan that is given in Fig 2.1.

In sampling 16 figurines were selected. The selection of the figurines was made on the basis of their physical appearance and durability conditions, i.e. choosing broken fragments were chosen in order to not damage well-preserved figurines. The samples are from different trenches in lower terrace as well as one sample from upper terrace and represent the time period when the figurines are dated, approximately from late 7th century to middle of 6th century B.C.. To obtain more homogeneity for the determination of chemical composition of figurines, samples were taken from 2 different places of the figurines.

Names and descriptions of samples are given in Table 2.5.

Table 2.5 Names and brief descriptions of samples

Sample	Sub samples	Nomenclature	Archaeological Description	Visual Description
1	1-2	EMLT28B.3	ST02 I 8B.28B.3 (A-B)	Broken fragment
2	3-4	EMLT23.9	ST02 I 8B.23.9 (A-B)	Broken fragment

3	5-6	EMLT16A.11-a	ST02 I 8B.16A.11 (A-B)	Body fragment
4	7-8	EMLT16A.11-b	ST02 I 8B.16A.11 (C-D)	Leg fragment
5	9-10	EMLT18.4	ST02 I 8B.18.4 (A-B)	Fragment belongs to a lion figurine
6	11-12	EMLT10.26	ST01 I 8B.10.26 (A-B)	Body fragment
7	13-14-15	EMLT16.148	ST00 K 8C.16.148 (A-B-C)	Body fragment
8	16-17	EMLT16.151	ST00 K 8C.16.151 (A-B)	Broken fragment
9	18-19-20	EMLT16.152	ST00 K 8.C.16.152 (A-B-C)	Body fragment
10	21-22	EMUT18V	ST00 D 8A.18.V (A-B)	Body fragment
11	23-24	EMLT4.65	ST99 I 9B.4.65 (A-B)	Leg fragment
12	25-26	EMLT4.64	ST99 I 9B.4.64 (A-B)	Broken fragment
13	27-28	EMLT3.17	ST99 I 9B.3.17 (A-B)	Body fragment
14	29-30	EMLT9.21	ST99 K 8C.9.21 (A-B)	Leg fragment
15	31-32	EMLT2.17	ST99 I 9B.2.17 (A-B)	Leg fragment
16	33-34	EMLT4	ST99 I 9B.4 (A-B)	carbonate stone

EMECİK - SARI LİMAN ARKAİK TAPINAK

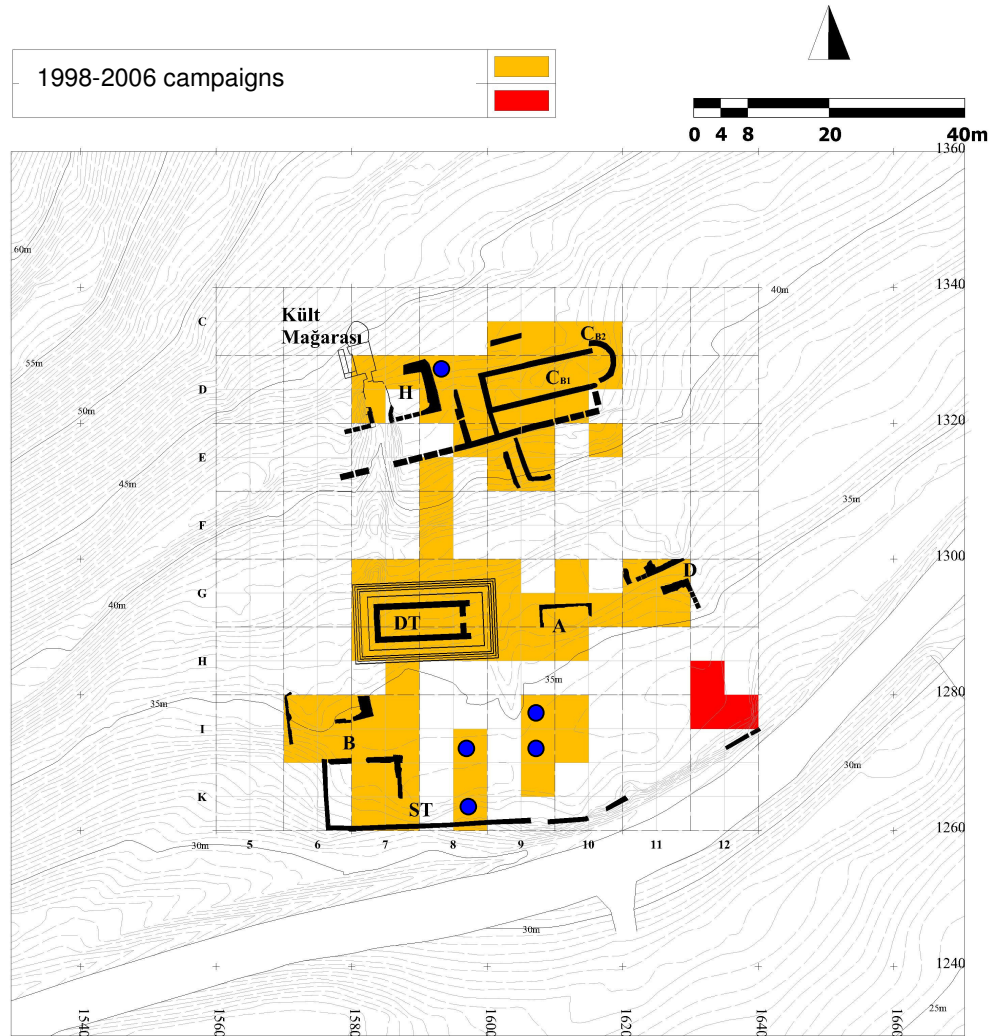


Fig.2.1. Plan of Emecik excavation [TAÇDAM archive], Blue dots show the locations from where the sampled figurines were obtained

2.3.2. Geological Samples from Datça Peninsula

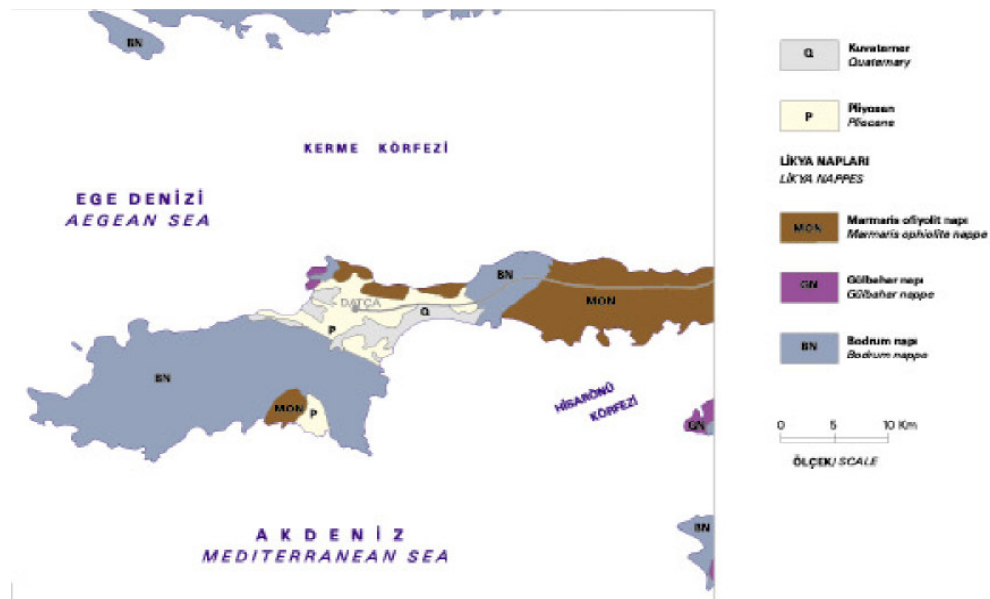


Figure 2.2. Map of Datça peninsula, Tectonic units MTA 1997

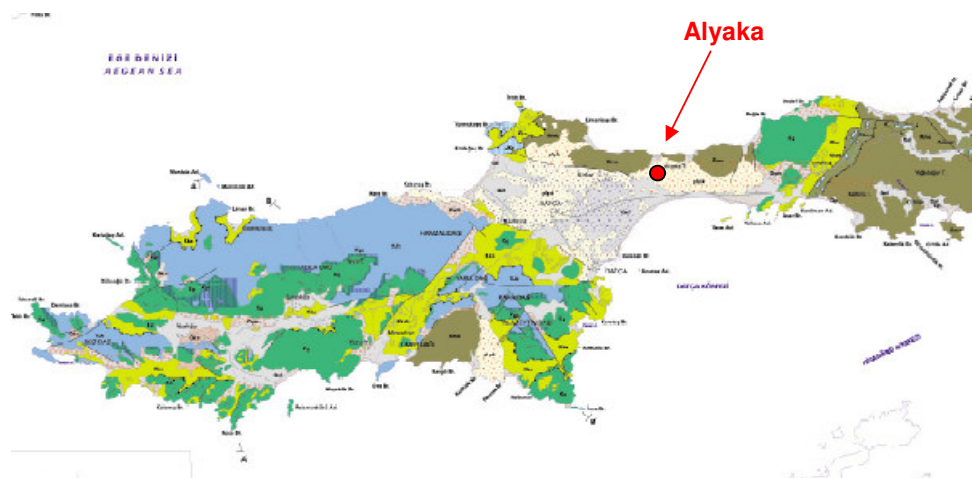


Figure 2.3. Geological map of Datça peninsula, MTA 1997 1:100.000, TRJK: Kayaköy dolomite; Kmo: Marmaris peridotite; Kg: Göçgediği Formation: micrite, cherty micrite, calciturbidite; Kka: Karaböğürtlen formation: sandstone, claystone, siltstone etc.; Kkak: limestone member: cherty limestone, calciturbidite; pilyık: Yıldırımılı continental formation; pilyid: Yıldırımılı marine formation; Qp: beach deposits; Qym: slope debris; Qal: alluvium

The rock units exposing in the Datça peninsula can be grouped into basement and cover rock units [48, 57]. The tectonic and geological maps of Datça peninsula are given in Fig.2.2. and 2.3.

Basement units are composed of ophiolite and ophiolitic *mélange*, carbonates and blocky *flysch* [48]:

Ophiolite and ophiolitic mélange units are mostly exposed in the south, to the east of Mesudiye along the coastline to the north of Kızlan village and the east around Emecik [48].

Carbonates start with massive carbonates at the bottom and continue with radiolarite-chert and at the uppermost levels it is represented by cherty limestone [48]. Massive carbonates are grayish in color and composed of thick layered, crystallized limestone, dolomite and platform carbonates, which are represented by breccia limestone. The outcrops of massive carbonates occur around Mersincik, Hamzalıdağ, Cumalı, around Kargı, Datça, Hızırşah and Emecik, Kocadağ, Kızılağaç Tepe. The radiolarite-chert levels are conformable with the lower massive carbonates. Pink to red, green colored, marly-cherty levels of this unit is from middle-late Jurassic. The cherty limestone consists of whitish colored, well layered, chert nodular or layered micritic limestone. The outcrops of the unit appear around Datça, Emecik, Kızılağaçtepe, Cumalı, Örencik, Knidos, Palamut bükü. The age of the unit has been estimated as late- Jura- early Maestrichtian.

Blocky flysch outcrops around Murdala, Mersincik bays, Knidos, Cumalı, Palamutbükü, Hızırşah Tepe and Kocadağ [48]. At the bottom, the unit starts with thin marl and clayey limestone, and continues upward with conglomerate and siltstone levels. The age of the unit has been accepted as upper Cretaceous-early Eocene.

Cover units are consisted of Yıldırımli formation, quaternary units, volcanics, hanging terrace deposits, talus and alluvial fan deposits, beach conglomerate, hanging beach conglomerates, beach sand and alluvium [48].

Late Pliocene aged, marine and continental Yıldırımli formation outcrops widely around Reşadiye, Hızırşah, Kızlan settlements and Körmen bay. The unit is

In order to make comparison with Cypriote geological structure samples from 3 different modern quarries in Cyprus were also collected. The geological map of Cyprus is given in Fig.2.4. and the details about these samples are given in Table 2.3.2.

Table 2.6. Names and description of geological samples

Name	Description
CD	Samples from Alyaka – Datça quarry
CC 1	Samples from Değirmenlik, Cyprus
CC 1a	Samples from Değirmenlik, Cyprus
CC2	Samples between Değirmenlik and Güngörköy
CC3	Samples from Güngörköy
CC4	Samples from Taşkent

2.4. Procedures

2.4.1. Microwave Assisted Dissolution

In the microwave acid dissolution applied three replicates of sample were placed into a PTFE vessel and the acid mixture was added. The composition of the acid mixture is given in below:

MW 200 mg samples 3.0 ml 65% HNO₃ + 3.0 ml 40% HF + 3.0 ml HCl

The microwave-heating program applied to samples is shown in Fig. 2.5. When the program is completed, solutions in PTFE vessels were kept at room temperature for one night and then evaporated to dryness on hot plate at 80°C in order to drive out excess HF. Dried mass was dissolved with 3.0 ml 65% HNO₃, and evaporated to dryness once more. The residue was dissolved with 2.0 ml 65% HNO₃ and transferred into PTFE containers. After filtration through a membrane filter under

vacuum, samples were diluted to the mark 50 ml with 1% HNO_3 . Blank was prepared in the same way as samples. ⁹

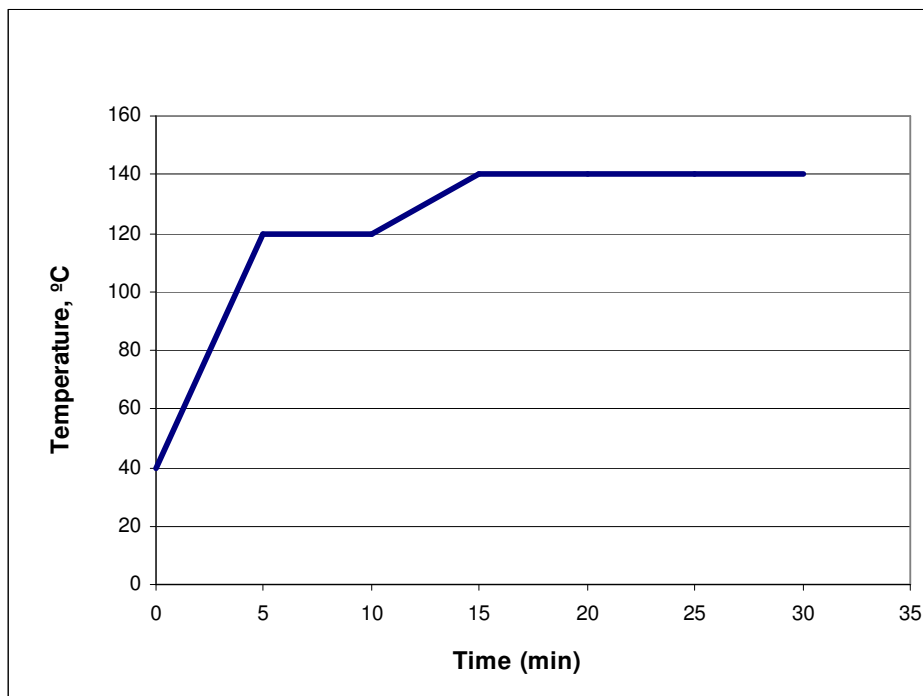


Figure 2.5. Microwave heating program

2.4.2. Dissolution by Fusion

Two reflux materials, LiBO_2 and $\text{Li}_2\text{B}_4\text{O}_7$, were used for dissolution by fusion. Three replicate measurements were performed: 0.200 g of sample was weighed and placed in the crucible. 1 g of LiBO_2 - $\text{Li}_2\text{B}_4\text{O}_7$ mixture (4:1) was added to the crucible and solid material was mixed carefully with a PTFE rod. The same procedure was followed for the blank solution.

The crucibles were heated in a muffle furnace at 1050°C for 1 hour. The fused glass was cooled and transferred into a PTFE beaker. The beaker was placed on magnetic stirrer after adding about 50 ml water and 1.5 ml concentrated HNO_3 . The

crucible was rinsed with 5 mL of 20 % HNO₃ and the contents were poured into the beaker. The beaker was covered with a watch glass and the contents were stirred until all the melt dissolved. After filtration through a membrane filter under vacuum the solution was diluted to 100 ml or 250 ml in a plastic volumetric flask with HNO₃ of about 1% final concentration.

2.5. Quantitative Analysis

2.5.1. ICP – OES

Fe, Mg, Sr, Ba contents of SRM NIST1d and figurine samples with geological samples were determined by ICP – OES using original solutions. For the determination of Mg and Fe standard addition method was applied. The wavelengths were chosen in interference free spectral regions with appropriate sensitivity for the concentration values obtained after dilution. Table 2.5 shows the wavelengths used in the analysis. After completion of the analysis, the data were transferred to Microsoft Excel prior to processing.

Table 2.7. Chosen wavelengths in ICP-OES, Leeman DRE.

Element	Wavelength (nm)
Fe	259.940
Mg	279.553
Sr	407.771
Ba	455.403

2.5.2. ICP – MS

La, Ce, Nd, Sm, Eu, Yb and Lu contents of SRM IGS 40 and NCS DC 73306 and figurine samples with geological samples were determined by ICP – MS. Below mentioned isotopes were selected for analysis:

Element	Nominal Mass	Mass (amu)	Abundance
La	139	138.9064	99.91
Ce	140	139.9054	88.48
Nd	146	145.9131	17.26
Eu	151	150.9199	47.77
Sm	152	151.9197	26.63
Yb	174	173.9389	31.84
Lu	175	174.9408	97.40

Due to low concentration of REE and high concentration of Ca in NCS DC 73306, standard addition method was applied and gave appropriate results for the determination of REE. Since NCS DC 73306 resembles the matrix for the figurines and the geological samples better than the REE ore IGS 40, standard addition method was also applied for analysis of the real samples.

2.6. Thin-section Analysis

In order to investigate mineralogy and the texture of figurines, one figurine fragment, EMUT18V was prepared and observed using an optical microscope. To make comparison thin-section of a sample from Alyaka quarry, CD was also prepared and observed. Thin section analyses were carried out by the Thin Section Laboratory of the Geological Engineering Department in METU. The optical examination was carried out in the laboratories of Geological Engineering Department of METU. The photomicrographs of the samples are given in Fig.2.6, 2.7, 2.8, 2.9.

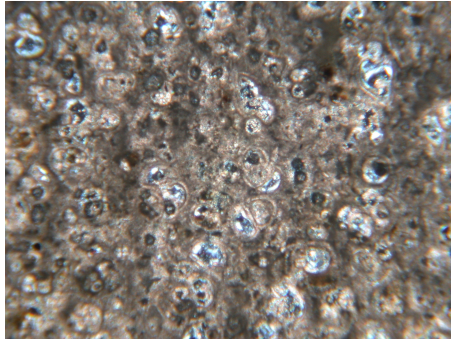


Fig.2.6. Thin-section photomicrograph of EMUT 18V foraminiferal limestone (PPL, objective x4)

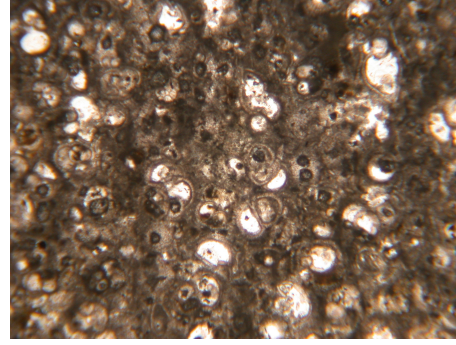


Fig.2.7. Thin-section photomicrograph of EMUT 18V, foraminiferal limestone (XPL, objective x4)

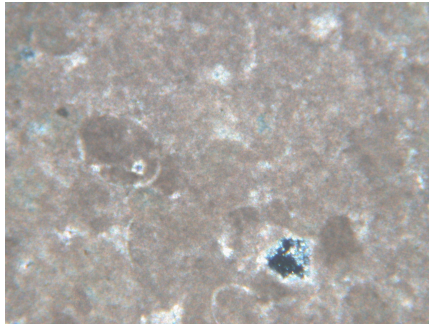


Fig.2.8. Thin-section photomicrograph of sample CD, a lithographic limestone (PPL, objective x4)

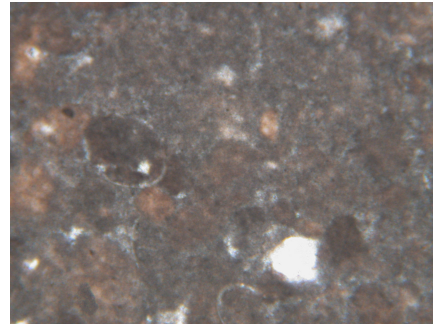


Fig.2.9. Thin-section photomicrograph of sample CD, a lithographic limestone (XPL, objective x4)

2.7 X-ray Diffraction Analysis

In order to identify the minerals, X-Ray powder diffraction (XRD) analyses of a figurine fragment, EMUT18V and a quarry sample from Alyaka, CD were carried out. XRD traces of samples were obtained at the Geological Engineering Department in METU by using Rigaku Ultima D/MAX 2200/PS XRD instrument operated at 40 kV / 4 mA using CuK α radiation. XRD traces of samples are given in Fig.2.10 and Fig.2.11.

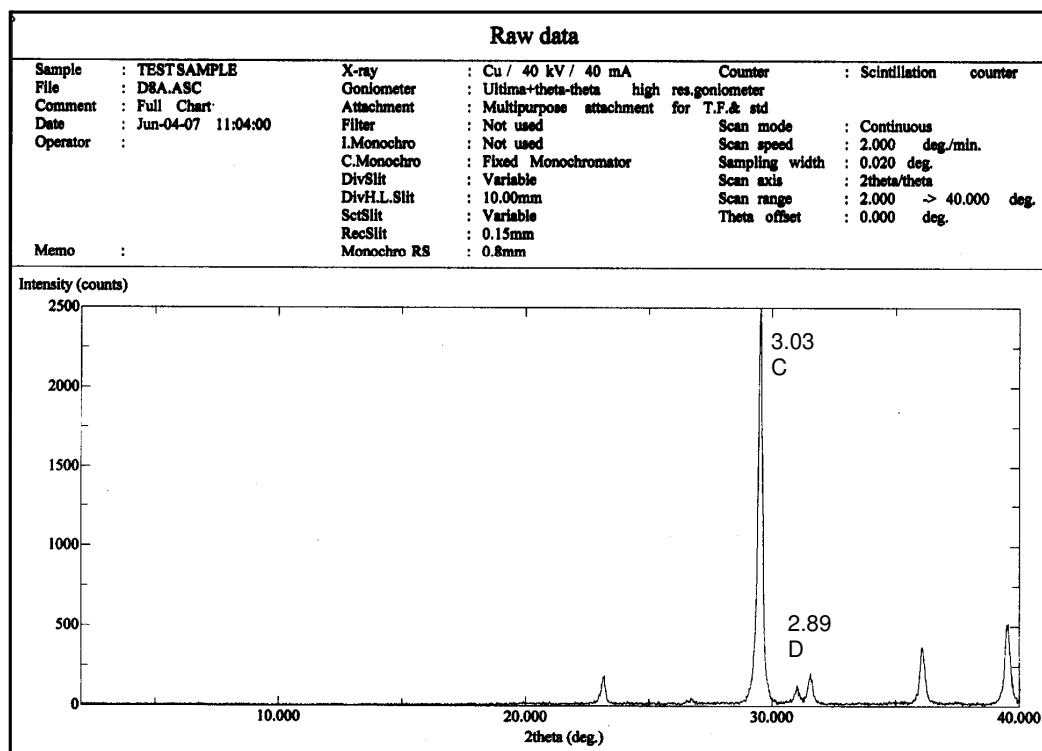


Fig.2.10. XRD trace of EMUT 18V indicating the presence of calcite C, dolomite D

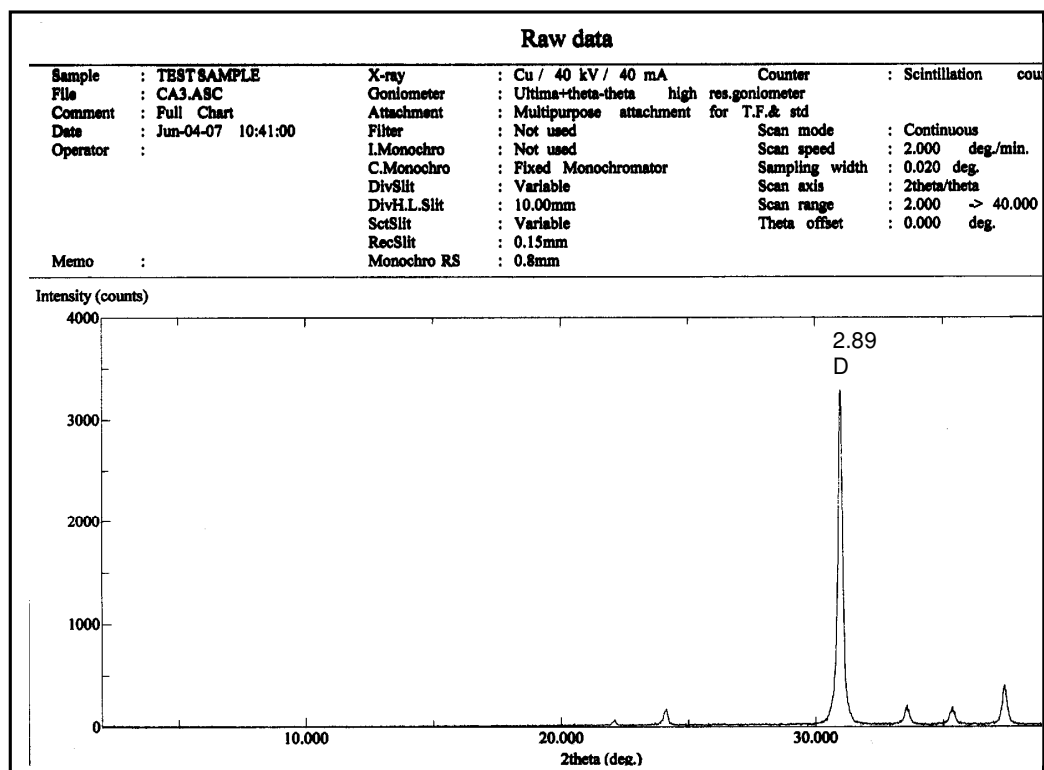


Fig.2.11. XRD trace of CD indicating the presence of dolomite D

CHAPTER 3

RESULTS AND DISCUSSION

3.1. Optimization of ICP – OES Conditions

Optimization conditions were done for Rf power, coolant gas flow rate, and pump rate since these parameters are the most effective factor of ICP – OES for analysis. Optimum values given in manual of instrument are used for other parameters such as auxiliary gas flow and nebulizer flow rate. RF power of 1.3 Kw was kept during the analyses to maintain the long term stability, robustness, of plasma.

3.2. Evaluation of Different Dissolution Procedures

Although fusion with lithium metaborate- lithium tetraborate is generally found to be the most suitable method for obsidian samples, this dissolution technique has considerable disadvantages especially as regards ICP – MS application. Therefore the most efficient dissolution of carbonate rock by acid mixture and microwave heating was aimed in this thesis. However, both dissolution methods were performed for SRM's in order to make comparisons.

3.3. Results of Analysis of Reference Materials

Results of microwave assisted digestion and dissolution by fusion procedures of NIST1d geological sample by ICP - OES are given in Table 3.1.

Table 3.1 Results for NIST 1d Argillaceous, Limestone

Found*	BaO	SrO	Fe ₂ O ₃	MgO
Fusion	0.0037± 0.0001	0.0295± 0.0007	0.3211± 0.0041	0.299 ± 0.006
MW	0.0035 ± 0.0001	0.0310± 0.0008	0.3160± 0.0069	0.290 ± 0.011
certified values	0.0033±0.0011	0.0303± 0.0010	0.3191± 0.0068	0.301± 0.010

* Values are in % w/w.

Results of microwave assisted digestion and dissolution by fusion procedures of IGS 40 and NCS DC 73306 by ICP - MS are given in Table 3.2 and in Table 3.3 respectively.

Table 3.2 Results for IGS 40

	Found*	Certified*
La ₂ O ₃	2.42 ± 0.01	2.41-2.45
CeO ₂	3.08 ± 0.03	3.79-4.06
Eu ₂ O ₃	0.009 ± 0.001	0.008-0.012
Nd ₂ O ₃	0.92 ± 0.07	0.95-0.99
Sm ₂ O ₃	0.061 ± 0.004	0.057-0.063

* Values are in % w/w

Table 3.4. Results for NCS DC 73306

Found	La mg/kg	Ce mg/kg	Nd mg/kg	Sm mg/kg	Eu mg/kg	Yb mg/kg	Lu mg/kg
Fusion 100mL	13.2±0.4	25.1±0.5	10.1±0.3	2.1 ± 0.1	0.45± 0.02	0.77± 0.02	0.10± 0.01
Fusion 250 mL	14.7± 0.7	21.9± 1.1	11.4± 0.3	ND	ND	ND	ND*
MW	12.2± 0.6	26.8± 0.9	10.3± 0.3	2.2± 0.1	0.47± 0.02	0.74± 0.04	0.10± 0.01
certified values	15± 5	25± 4	12.0± 1.4	2.4± 0.3	0.51± 0.07	0.90± 0.16	0.14± 0.04

*ND not detected

3.4. Results of Analysis of Figurines and Geological Samples

Thirteen figurine samples and four different geological samples were dissolved in microwave oven according to above-mentioned procedures Chapter 2.4 and all were analyzed with ICP – OES for trace elements and with ICP – MS for REE. Results are given in Tables 3.4 and 3.5

Table 3.3 Results for figurines and geological samples with ICP – OES

Samples	MgO %	Fe ₂ O ₃ %	Sr mg/kg	Ba mg/kg
EMLT16A.11-a	0.37±0.01	0.28±0.01	330±5	17.2±0.23
EMLT16.A11-b	0.45±0.01	0.43±0.01	590±10	20.4±0.27
EMLT2.17.	0.41±0.01	0.20±0.01	500±8	15.9±0.23
EMUT18V	0.70±0.01	0.39±0.01	570±9	13.3±0.18
EMLT4.65	0.31±0.01	0.45±0.01	590±10	17.9±0.24
EMLT16.148	0.43±0.01	0.32±0.01	660±8	19.4±0.26
EMLT16.151	0.45±0.01	0.39±0.01	640±11	18.1±0.24
EMLT16.152	0.34±0.01	0.30±0.01	580±10	17.2±0.23
EMLT 28B.3	0.72±0.01	0.44±0.01	560±9	21.9±0.29
EMLT9.21	0.58±0.01	0.42±0.01	560±9	82.3±1.10
EMLT18.4	0.53±0.01	0.49±0.01	700±12	23.5±0.32
EMLT10.26	0.68±0.01	0.24±0.01	480±8	17.2±0.23
EMLT4	0.29±0.01	0.31±0.01	390±6	20.9±0.28
CD	3.63±0.07	0.35±0.005	250±4	20.9±0.28
CC1	0.35±0.01	0.0060±0.0001	120±2	ND
CC1a	0.30±0.01	0.0090±0.0001	110±2	ND
CC3	0.76±0.02	0.0100±0.0001	220±4	ND
LOD µg/kg	3.15	2.74	3.45	7.5

* ND not detected

Table 3.5. Results for figurines and geological samples with ICP – MS

Samples	La mg/kg	Ce mg/kg	Nd mg/kg	Sm mg/kg	Eu mg/kg	Yb mg/kg	Lu
EMLT16A.11-a	1.67±0.01	1.88±0.01	1.64±0.02	0.31±0.01	0.072±0.001	0.140±0.001	ND
EMLT16.A11-b	2.09±0.01	2.07±0.01	2.11±0.02	0.40±0.01	0.087±0.001	0.160±0.002	ND
EMLT2.17.	1.55±0.01	1.62±0.01	1.54±0.02	0.36±0.01	0.074±0.001	0.140±0.001	ND
EMUT18V	1.05±0.01	1.24±0.01	0.96±0.01	0.21±0.01	*	*	ND
EMLT4.65	1.95±0.01	1.85±0.01	1.92±0.02	0.33±0.01	0.079±0.001	0.170±0.002	ND
EMLT16.148	1.96±0.01	2.18±0.02	1.93±0.02	0.32±0.01	0.078±0.001	0.190±0.002	ND
EMLT16.151	2.58±0.01	2.81±0.02	2.46±0.02	0.51±0.01	0.12±0.001	0.230±0.002	ND
EMLT16.152	1.85±0.01	1.83±0.01	1.77±0.02	0.33±0.01	0.071±0.001	0.100±0.001	ND
EMLT 28B.3	2.50±0.01	2.49±0.02	2.34±0.02	0.45±0.01	0.11±0.001	0.230±0.002	ND
EMLT9.21	2.50±0.01	2.70±0.02	2.29±0.02	0.43±0.01	0.10±0.001	0.130±0.002	ND
EMLT18.4	1.41±0.01	1.41±0.01	1.33±0.01	0.25±0.01	0.062±0.001	0.130±0.002	ND
EMLT10.26	2.67±0.01	2.79±0.02	2.64±0.03	0.52±0.01	0.14±0.001	0.230±0.002	ND
EMLT4	1.84±0.01	2.04±0.01	1.79±0.02	0.35±0.01	0.085±0.001	0.170±0.002	ND
CD	1.56±0.01	2.62±0.02	1.29±0.01	0.22±0.01	*	*	ND
LOD µg/kg	11.58	1.88	5.81	10.86	8.92	12.19	5.75

*ND not detected

3.5. Results of Thin-section and XRD Analyses

Only one of the figurine samples, EMUT18V, was subjected to thin-section microscopic analysis; it was found to be made of foraminiferal limestone. Inside of the fossils sometimes is filled by chert. In XRD analysis of the figurine sample calcite appeared to be the major mineral and trace quantities of dolomite may also be present. The geological age of the limestone is most probably Tertiary (Miocene/Pliocene?) and deposited in pelagic environment.

The sample of the Alyaka, Datça quarry exhibit micritic texture with pores and few fossils remain as seen in thin-sections. There is also iron-oxidation, although it is not very widespread. Dolomite as detected by XRD analyses is the only mineral. The depositional environment of this limestone may be also a pelagic environment.

3.6. REE Patterns and M-bird-grams of Figurines and Geological Samples

REE patterns and M-bird-grams of the samples were constructed by using ratio of sample values to C1 chondrite values for each REE [34]. Chondrite values of the elements are given in Table 3.6.

Table 3.6 Values of REE, Ba and Sr in C1 Chondrite

Element	mg/kg
Ba	2.41
La	0.237
Ce	0.612
Sr	7.26
Nd	0.467
Sm	0.153
Eu	0.058
Yb	0.170

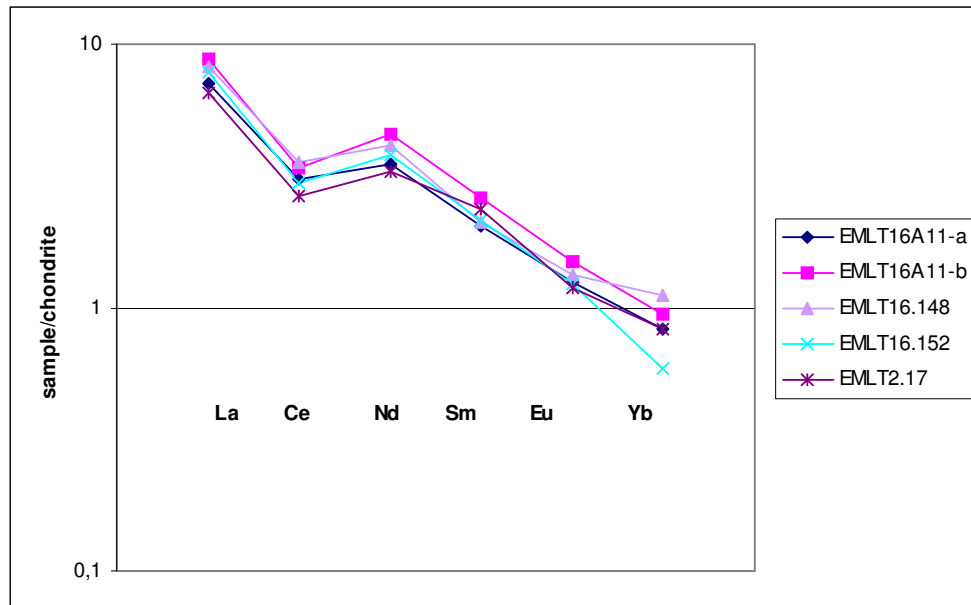


Figure 3.1. REE patterns of Emecik figurines, EMLT16A11-a, 16A11-b, 16.148, 16.152 and 2.17

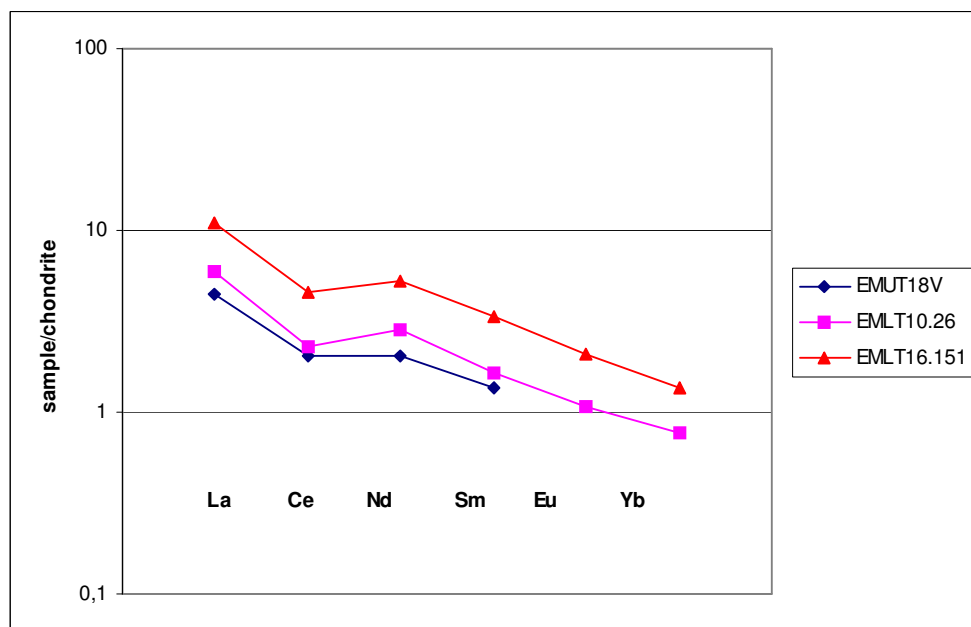


Figure 3.2. REE patterns of Emecik figurines, EMUT18V, EMLT10.26 and 16.151

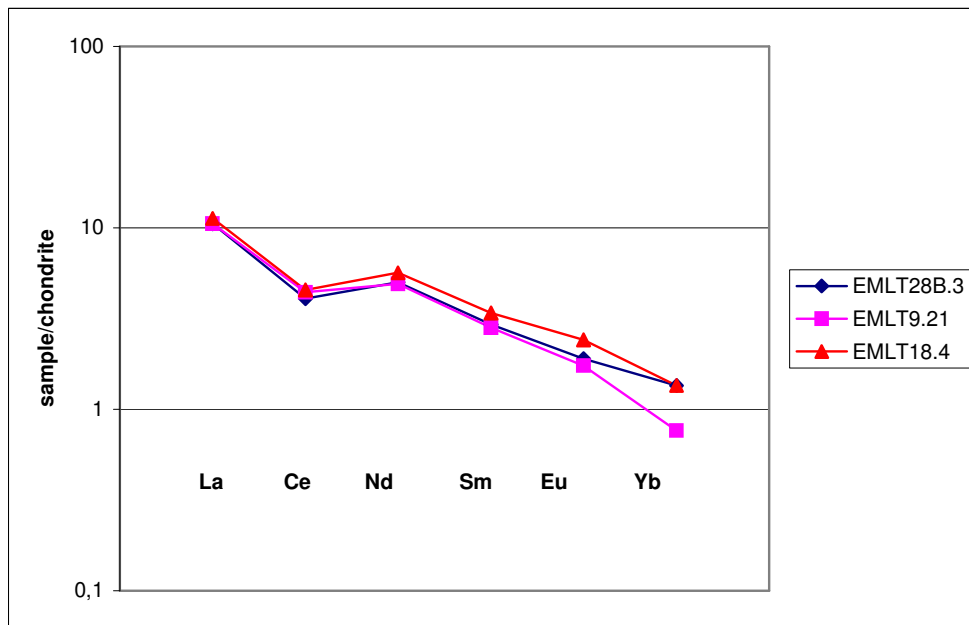


Figure 3.3. REE patterns of Emecik figurines, EMLT28B.3, 9.21 and 18.4

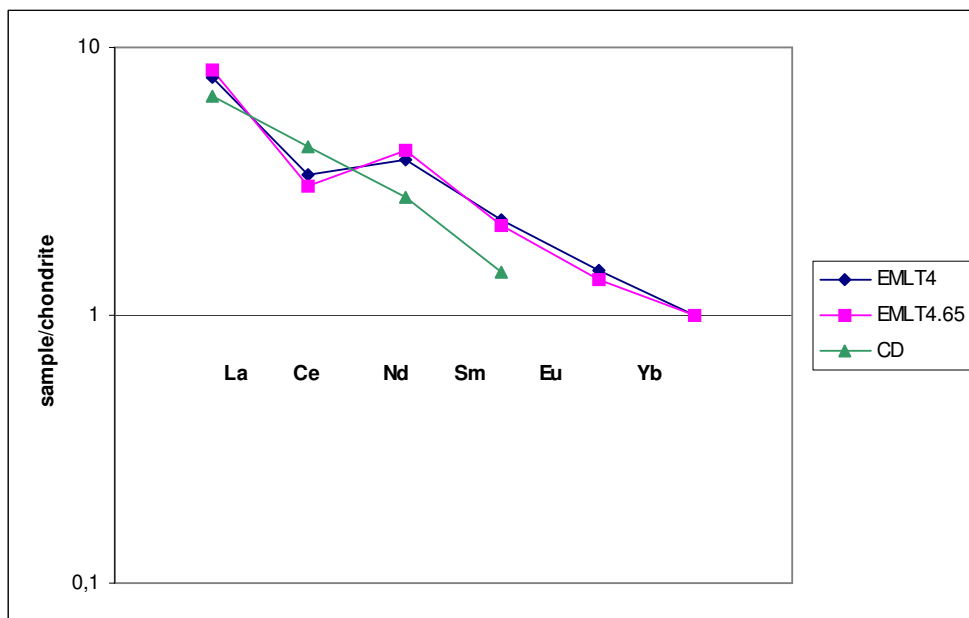


Figure 3.4 REE patterns of the figurine EMLT4.65, the stone sample EMLT4 and the geological sample CD

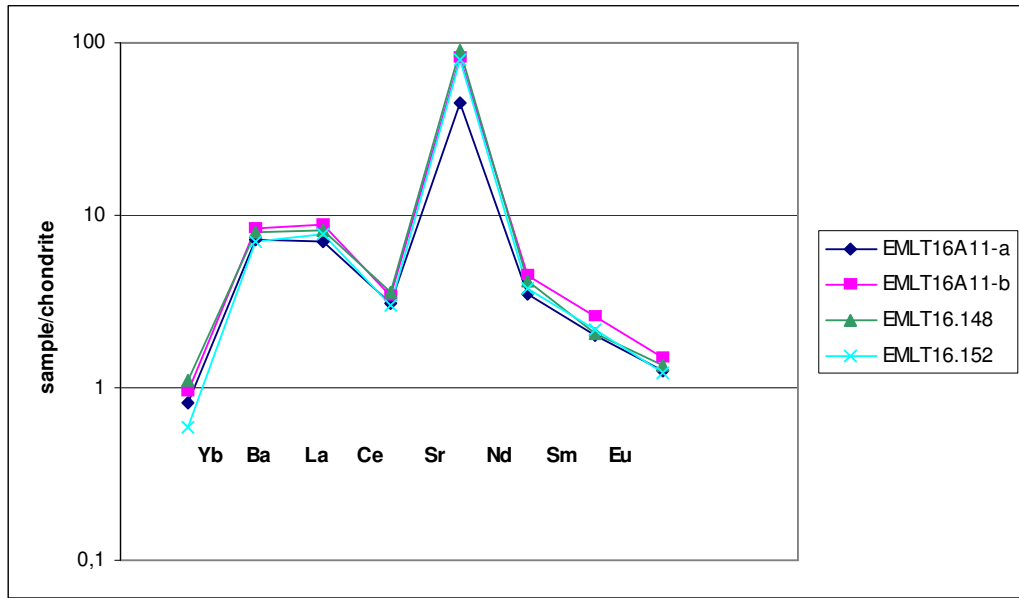


Figure 3.5. M-bird-grams of Emecik figurines, EMLT16A11-a, 16A11-b, 16.148 and 16.152

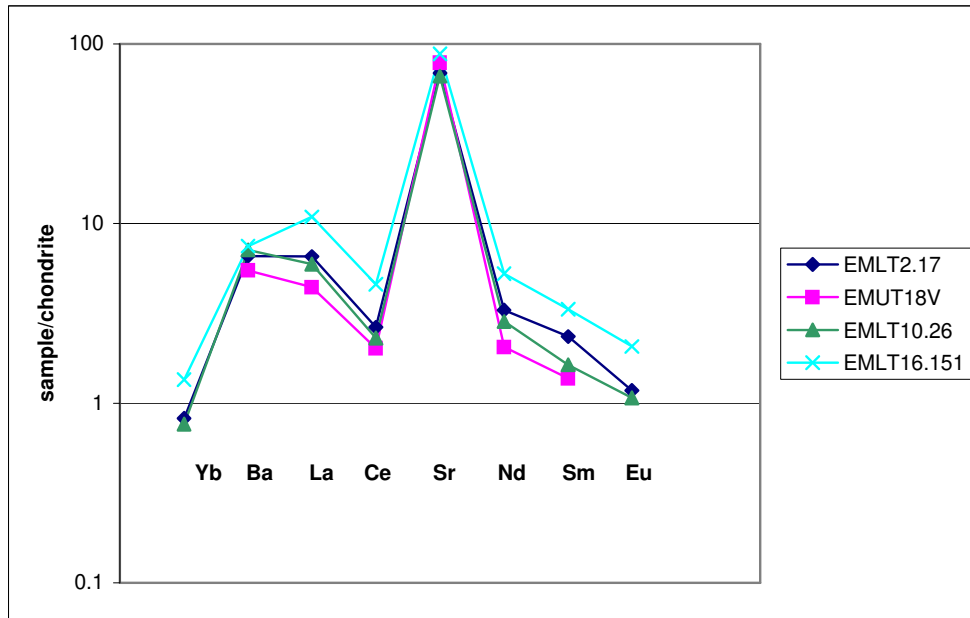


Figure 3.6. M-bird-grams of Emecik figurines, EMLTU18V, EMLT2.17, 10.26 and 16.151

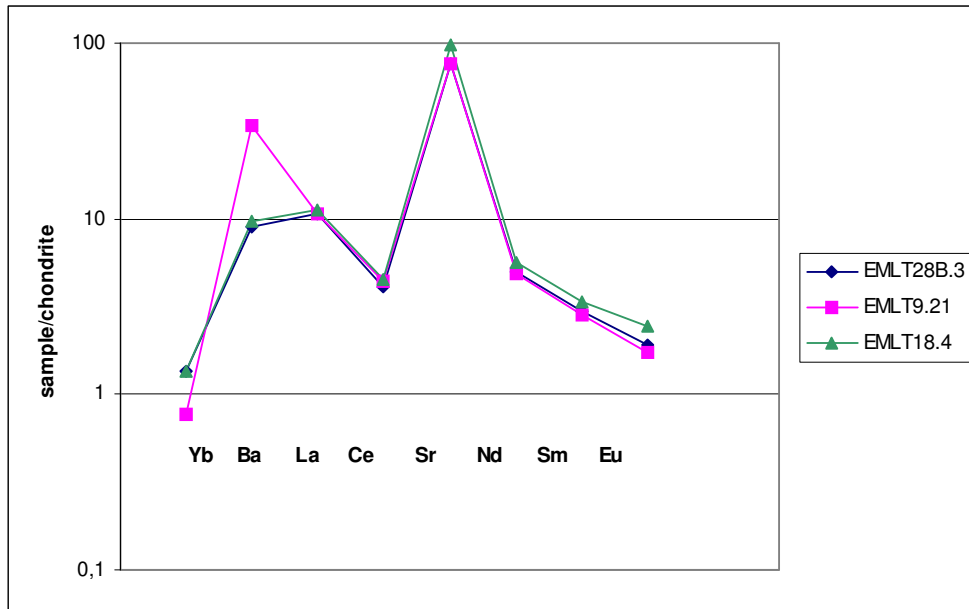


Figure 3.7. M-bird-grams of Emecik figurines, EMLT28B.3, 9.21 and 18.4

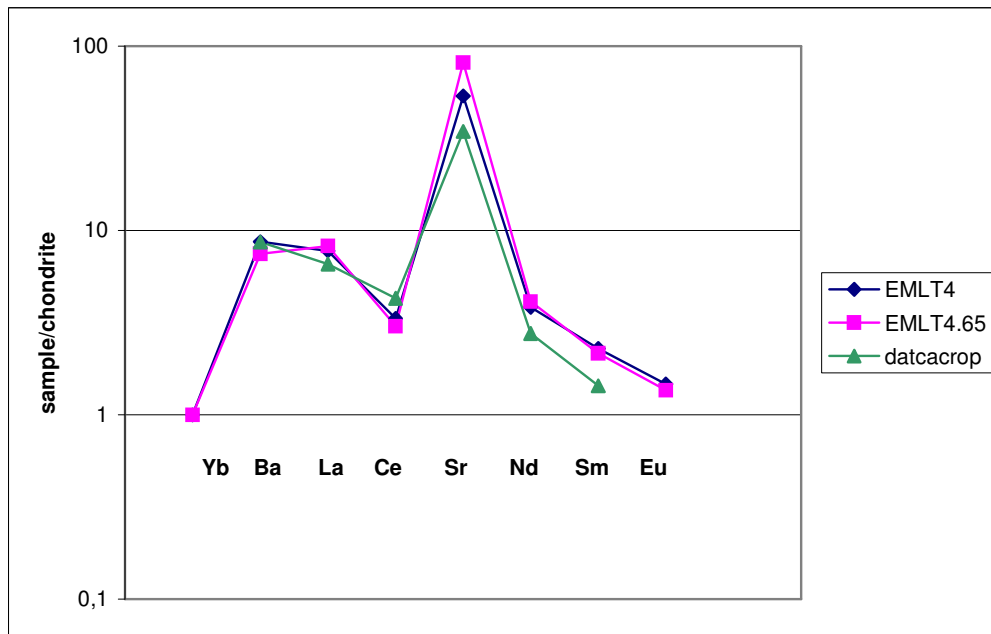


Figure 3.8 M-bird-grams of the figurine EMLT4.65, the stone sample EMLT4 and the geological sample CD

3.7. Element Ratios and Binary Diagrams of Figurines and Geological Samples

La_{cn}/Yb_{cn} , La_{cn}/Sm_{cn} ratios for TREE fractionation and LREE fractionation respectively, beside Eu/Ce ratio and evaluated Ce anomalies of figurine and quarry samples are determined and are given in Table 3.7.

Table 3.7. TREE, LREE fractionations, Eu/Ce ratio and Ce anomalies of figurine and quarry samples

Samples	La_{cn}/Yb_{cn}	La_{cn}/Sm_{cn}	Eu/Ce	Ce/Ce^*
EMLT16A11-a	11.93	0.82	0.038	0.39
EMLT1611-b	13.06	0.79	0.042	0.46
EMLT16.148	10.32	0.94	0.036	0.52
EMLT16.152	18.50	0.86	0.039	0.46
EMLT2.17	11.07	0.66	0.046	0.48
EMUT18V	-	0.76	-	0.56
EMLT10.26	10.85	0.86	0.044	0.47
EMLT16.151	11.22	0.77	0.043	0.51
EMLT28B.3	10.87	0.85	0.044	0.47
EMLT9.21	19.23	0.89	0.037	0.51
EMLT18.4	11.61	0.79	0.050	0.49
EMLT4	10.82	0.80	0.042	0.52
CD	-	1.08		0.81

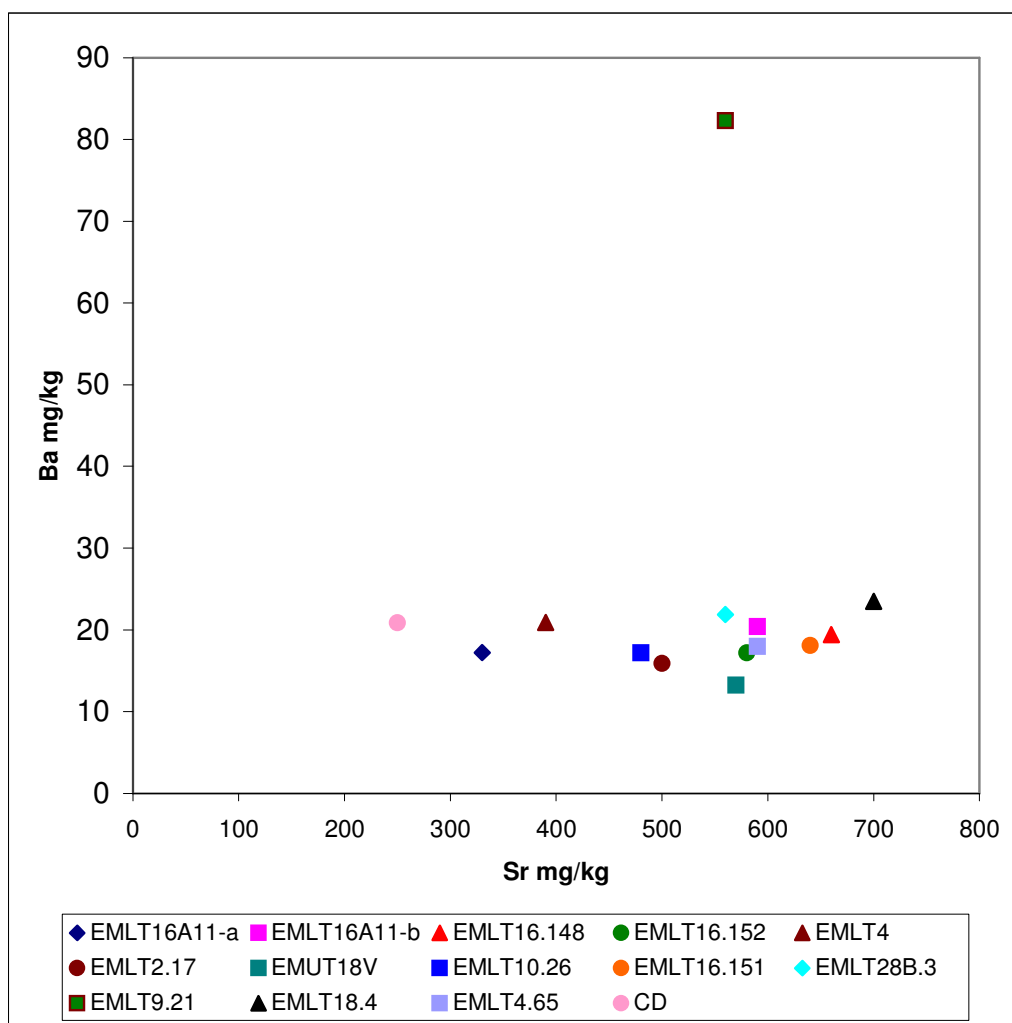


Fig.3.9. Ba vs Sr binary diagram of figurines

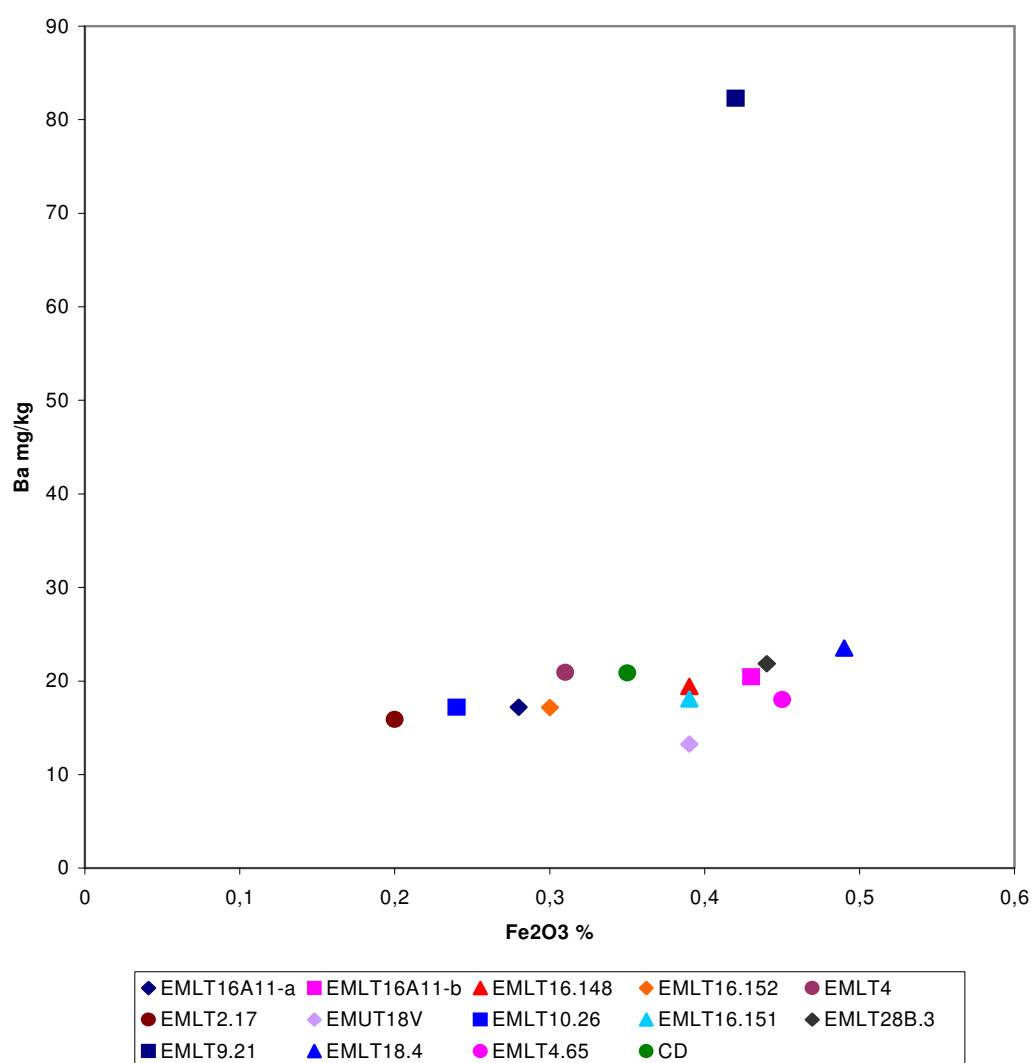


Fig.3.10. Ba vs Fe₂O₃ binary diagram of figurines

CHAPTER 4

CONCLUSION

In this study the applicability of the inductively coupled plasma mass spectrometry, ICP-MS and inductively coupled plasma optical emission spectrometry, ICP-OES for the provenance analysis of some archaeological samples, figurines found in Emecik excavations and geological samples from modern quarries from Datça and Cyprus were investigated.

The dissolution method was developed using three different standard reference materials, NIST 1d, NCS DC 73306 and IGS 40. Thirteen figurines samples were chosen for analysis out of sixteen samples, because three of them were collected from deteriorated surfaces of the samples, and samples from two modern quarries in Cyprus could not be dissolved by the method developed in this study.

According to the results, Mg content of geological samples from Alyaka, Datça and the figurines is different and this difference can also be observed from M-bird-grams and REE patterns, although Fe, Sr and Fe concentrations or REE concentration are similar. Results of XRD analyses of one figurine fragment, EMUT18V and Alyaka quarry sample are in accordance with ICP-OES results for Mg content. Alyaka quarry sample is appeared to be composed of dolomite minerals, although the figurine were made of limestone composed of calcite minerals. Thin-section analysis indicated that the figurine, EMUT18V was made of foraminiferal limestone, which shows typical texture of this type of limestone, and the stone from Alyaka is lithographic limestone.

Ce anomaly, Ce/Ce^* , for figurines are determined to be moderate while geological samples from Alyaka show no negative Ce anomalies. Moreover, TREE and LREE fractionations of Alyaka quarry samples is found to be bigger than that of figurines, while total REE concentrations of figurines are higher than the total REE concentration of Alyaka samples. Mg content of geological samples from Cyprus is similar to figurines; however their other trace element concentrations are different and REE are found to be below the detection limit.

Binary diagram, REE patterns and M-bird-grams of the stone sample found in Emecik and figurines have good correlation. Only one of the figurine samples has a higher Ba content.

Finally, the figurines from Emecik were definitely not of Alyaka quarry or of the Taşkent, Güngörköy and Değirmentepe quarries. By foraminifera remains the limestone that the figurines were made of could be dated to Tertiary period and is deposited in pelagic environment. The figurines have a REE pattern that is now understood to be typical with a certain Ce anomaly and could be discriminative for the Emecik figurines.

Further studies should continue in the light of these results, focusing on pelagic limestone sources and searching for the traces of ancient quarries from Tertiary period especially in Datça peninsula and including other figurines found both in Emecik, surrounding regions and in Cyprus.

REFERENCES

1. Martini M., Milazzo and Piacentini, M., *Proceedings of the International School of Physics*, IOS pres., Amsterdam (2004), pp 407-432.
2. Vito C.d, Ferrini V., Mignardi S., Piccardi L., Rosanna T., *Journal of Archaeological Science*, 2004, 31(10), 1391-1393.
3. Marinoni N., Pavese A., Bugini R., Silvestro G.d, *Journal of Cultural Heritage*, 2003, 3(4), 241-249.
4. Holmes, L.L., Harbottle, G., *Archaeometry*, 1994, 36 (1), 25-39.
5. Tuna N., Berges, D., *Kazı Sonuçları Toplantısı*, 2000, 22(2), 197-205.
6. Cornelius S., Hurlbut, Jr., Cornelis K., *Dana's Manual of Mineralogy*, Wiley, New York, (1977) pp 497-498.
7. Konrad B., Krauskopf, D.K.B., *Introduction to Geochemistry*, McGraw-Hill International Editions, Singapore (1995).
8. Blatt H., Middleton G., Murray R., *Origin of Sedimentary Rocks*, Prentice-Hall, New Jersey, (1972), pp 412-413.
9. Blatt H., *Sedimentary Petrology*, W.H. Freeman and Company, New York (1992).

10. Oates J.A.H., *Lime and Limestone*, Wiley-VCH, New York (1998).
11. Tucker M.E., *Sedimentary Petrology, An Introduction to the Origin of Sedimentary Rocks*, Blackwell Scientific Publications, London (1991).
12. Boynton, R.S., *Chemistry and Technology of Lime and Limestone*, John Wiley & Sons, New York (1966).
13. Durham R.J., *American Association of Petroleum Geologists Memoir*, 1962, 117, 108-121.
14. *CRC Handbook of Chemistry and Physics*, Chemical Rubber Co., Cleveland (1971).
15. Mellaart J., *Çatal Huyuk: A Neolithic Town in Anatolia*, McGraw Hill, London (1967).
16. Özdoğan M., Başgelen N. (eds.), *The Cradle of Civilization*, New Discoveries, Arkeoloji ve Sanat Yayınları, İstanbul (1999).
17. G. R. Tsetskhladze, et al. (eds.), *Periplous: Papers on Classical Art and Archaeology Presented to Sir John Boardman*, J.N.W. and Snodgrass, London, (2000), pp 153-162.
18. Polikreti K., Maniatis Y., Bassiakos Y., Kourou N., Karageorghis V., *Journal of Archaeological Sciences*, 2004, 31(7), 1015-1028.
19. Richter G., *Archaic Greek Youths*, Phaidon Press, London (1960).
20. Berges D., *Knidos, Beiträge zur Geschichte der archaischen Stadt*, Verlag Philipp von Zabern, Mainz am Rhein (2006).
21. Kourou N., Karageorghis V., Maniatis Y., Polikreti K., Bassiakos, Y., *Limestone Statuettes of Cypriote Type Found in the Aegean: Provenance Studies*, A.G. Leventis Foundation, Nicosia (2002).

22. Jenkins I., *American Journal of Archaeology*, 2001, 105 (2), 163-179.
23. Kourou, N. *Interconnections in the Mediterranean 16th-6th B.C. in Proceedings of the International Symposium held at Rethymnon, Crete*, 2002, Athens.
24. Tuna N., Berges D., *Kazı Sonuçları Toplantısı*, 2000, 22(2), 197-205.
25. Tuna N., Berges D., *Kazı Sonuçları Toplantısı*, 2001, 23(2), 89-99.
26. Tuna N., *Kazı Sonuçları Toplantısı*, 2002, 24(2), 41-46.
27. Berges, D., *Nürnberg Blätter zur Archäologie*, 1995/96, 12, 103-120.
28. http://www.tacdam.metu.edu.tr/index.php?option=com_content&task=view&id=21&Itemid=61 last accessed 14.06.2007
29. Holmes L.L., Harbottle G., *Gest*, 1994, 33 (1), 10-18.
30. <http://www.limestonesculptureanalysis.com/default.asp> last accessed 14.06.2007.
31. http://www.metmuseum.org/special/set_in_stone/index.asp last accessed 14.06.2007.
32. Bello M.A., Martin A., *Archaeometry*, 1992, 34.1, 21-29.
33. Harrell J.A., *Archaeometry*, 1992, 34.1, 195-211.
34. Waelkens M., Herz N., Moens L.(eds.), 1992, *Ancient Stones: Quarrying, Trade and Provenance – Interdisciplinary Studies on Stones and Stone Technology in Europe and Near East from the Prehistoric to the Early Christian Period*, Leuven University Press, Leuven (1992).

35. Lipin, B.R., McKay, G.A. (eds), *Geochemistry and Mineralogy of Rare Earth Elements*, Washington, 1989.
36. Jones, A.P., F. Wall, Williams, C.T. (eds) *Rare Earth Minerals: Chemistry, Origin and Ore Deposits*, New York (1996).
37. Cullers, R., *Chemical Geology*, 2002, 191, 305-327.
38. Roy P.D., Smyktaz-Kloss W., *Chmie der Erde*, 2007, 67(1), 55-68.
39. Bellanca A., Masetti D., Neri R., *Chemical Geology*, 1997, 141, 141-152.
40. Bolhar R., Kamber B.S., Moorbath S., Whitehouse M.J., Collerson K.D., *Geochimica et Cosmochimica Acta*, 2005, 69(6), 1555-1573.
41. Igarashi, K., Akagi, T., Fu, F., Yabuki, S., *Analytical Sciences*, 2003, 35, 441-445.
42. Ionov D., Harmer R., *Earth and Planetary Science Letters*, 2002, 198(3-4), 495-510.
43. Halicz L., Segal I., Yoffe O., *Geological Survey of Israel*, 1999, 14, 1579-1581.
44. Müller G., Friedman G. (eds), *Recent Developments in Carbonate Sedimentology in Central Europe*, Berlin, Springer-Verlag (1968).
45. Ayhan İ.A., *Provenance Studies in Obsidian Samples from Çatalhöyük Excavations*, M.Sc. Thesis, METU (2002).
46. Öztürk S., *Use of Solid Phase Extraction for Preconcentration of Rare Earth Elements: Provenance Studies In Çatalhöyük Obsidians*, M.Sc. Thesis, METU (2003).
47. Shields, G., Stille, P., *Chemical Geology*, 2001, 175 (1-2), 29-48.

48. Dirican M., *Geoarchaeometrical Study of Burgaz Area, Datça Peninsula*, Turkey M.Sc. Thesis, METU (2002).
49. Raut N.M., Huang Ls., Lin Kc., Aggarwal S.K., *Analytica Chimica Acta*, 2005, 530, 91-103.
50. Chang Q., Shinotsuka K., Shibata T., Yoshikawa M., Tatsumi Y., *Frontier Research on Earth Evolution*, 2004, 2, 1-4.
51. Elliott S., *Varian's ICP-MS at work*, 1997.
52. Housecroft C.E., Sharpe A.G., *Inorganic Chemistry*, Edinburgh, Pearson Education (2001).
53. Topp N.E., *The Chemistry of the Rare-Earth Elements*, Amsterdam, Elsevier (1965).
54. Spedding F.H., Daane A.H., *The Rare Earths*, London, John Wiley (1961).
55. Petrucic R.H., Harwood W.S., Herring F.G. *General Chemistry*, New Jersey, Prentice Hall (2002).
56. <http://www.soton.ac.uk/~imw/Cyprus-Akrotiri-Lake-Coast.htm> last accessed 14.06.2007
57. Kayan İ., *Ankara Üniversitesi Dil ve Tarih-Coğrafya Fakültesi Dergisi*, Ankara, Ankara Üniversitesi, 1988, 11 (11), 51-70.